Tampere University

Nina Terho

MODELLING THE SPREAD OF CYCLOTRON EXHAUSTS

Faculty of Engineering and Natural Sciences
Dissertation for a Masters Degree
Examiners: Professor Michiel Postema,
Medical Physicist Pasi Korkola
October 2022

DISCLAIMER

This is a hypothetical study that has been carried out solely for an educational purpose. The values used for calculations are pure estimates, and therefore the results may not represent a real situation in the environment of Tampere University Hospital.

ABSTRACT

Nina Terho: Modelling the Spread of Cyclotron Exhausts
Dissertation for a Masters Degree
Tampere University
Masters' Programme in Science and Engineering
October 2022

Cyclotrons are used to produce radioisotopes for radiopharmaceuticals in medical diagnosis and treatment. Because the produced isotopes are relatively short-lived, it is often required to produce them on the site they are further used. Following the operation, radioactive waste is always released into the atmosphere, and before starting such operation, the operator is required to show that the exhausts do not risk the population radiation safety. This dissertation studied the atmospheric spread of radionuclides in a schematic situation where a cyclotron operation would be launched at Tampere University Hospital (Tays), and because no complete calculation tool was available, one was created.

Radioactivity concentrations of ^{11}C and ^{18}F were modelled in the vicinity of the emission by applying a Gaussian dispersion model, assuming constant meteorological and source conditions, and neglecting terrestrial elevation. The maximum concentrations were determined at five heights above the ground in two release scenarios: 1) normal, continuous release and 2) instantaneous accidental leak. The results were applied for dose calculations to investigate the magnitude of radiation doses in the environment of the cyclotron.

The concentration profiles drawn in several planes showed that the maximum concentration moved towards the source and increased as the point of observation approached the release height. The dose calculations revealed that the maximum allowed dose was exceeded in both normal release and accidental leak scenarios at some calculation points. In each modelled scenario, the dose limit was exceeded only at the level of release height.

The outcome of this dissertation was a calculation tool using which a good estimate of the magnitude of the doses resulting from cyclotron operation at Tays was made. With the input parameter values used for the dose calculations, the maximum acceptable radiation dose was exceeded at some points at the height of release, which would limit placing high buildings in the vicinity of the exhaust chimney. The knowledge of the real future situation at Tays was limited, and therefore the nature of this study was entirely hypothetical.

Keywords: cyclotron-produced radiotracer, airborne radionuclide concentration, atmospheric dispersion modeling, Gaussian plume model, radiation dose calculation

TIIVISTELMÄ

Nina Terho: Syklotronista vapautuvien kaasumaisten päästöjen leviämisen mallinnus
Diplomityö
Tampereen yliopisto
Teknis-luonnontieteellinen diplomi-insinöörin tutkinto-ohjelma
Lokakuu 2022

Syklotroneja käytetään tuottamaan lääketieteellisessä diagnostiikassa ja hoidossa tarvittavia radiolääkkeitä. Syklotronilla tuotetut isotoopit ovat usein lyhytikäisiä, joten ne on valmistettava paikassa, jossa niitä edelleen käytetään. Isotooppien valmistuksessa vapautuu aina radioaktiivista jätettä ilmakehään, ja ennen toiminnan aloittamista toiminnanharjoittajan on osoitettava, etteivät päästöt vaaranna väestön säteilyturvallisuutta. Tässä diplomityössä tutkittiin radionuklidien leviämistä ilmakehässä kuvitteellisessa tilanteessa, jossa syklotronitoiminta aloitettaisiin Tampereen yliopistollisessa sairaalassa (Tays), ja koska valmista laskentatyökalua ei ollut saatavilla, sellainen luotiin.

^{11}C ja ^{18}F -isotooppien konsentraatioita mallinnettiin päästön läheisyydessä hyödyntäen Gaussista leviämismallia olettaen sääolosuhteet ja päästön ominaisuudet vakioksi, sekä jättäen maanpinnan korkeusvaihtelut huomioimatta. Maksimikonsentraatiot määritettiin viidellä korkeudella maanpinnan yläpuolella kahdessa päästöskenaariossa: 1) normaali, jatkuva päästö ja 2) hetkellinen onnettomuuspäästö. Tuloksia sovellettiin annoslaskelmiin väestön säteilyannoksen suuruuden arvioimiseksi syklotronin ympäristössä.

Eri tasoihin piirretyistä konsentraatioprofiileista nähtiin, että maksimikonsentraatio siirtyi kohti päästölähdettä ja sen arvo kasvoi havaintopisteen lähestyessä päästön korkeutta. Annoslaskelmat osoittivat, että suurin sallittu säteilyannos ylitettiin sekä normaalissa että onnettomuuspäästössä joissakin laskentapisteissä. Annosraja ylittyi vain päästön korkeuden tasossa jokaisessa mallinnetussa tilanteessa.

Tämän diplomityön tuotos on laskentatyökalu, jota hyödyntäen tehtiin hyvä arvio Taysin syklotronitoiminnan seurauksena aiheutuvien säteilyannosten suuruudesta. Annoslaskelmissa käytetyillä muuttujien arvoilla suurin sallittu säteilyannos ylittyi joissain pisteissä päästölähteen korkeudella, mikä rajoittaisi korkeiden rakennuksien sijoittamista poistopiipun läheisyyteen. Tietämys Taysin todellisesta tulevaisuuden tilanteesta oli rajallinen, minkä vuoksi tämän tutkimuksen luonne oli täysin hypoteettinen.

Avainsanat: syklotronilla tuotettu radioaktiivinen merkkiaine, ilman radionuklidipitoisuus, ilmakehän dispersion mallinnus, Gaussin vanamalli, säteilyannoslaskelma

PREFACE

Before you lies the dissertation for a master's degree "Modelling the Spread of Cyclotron Exhausts". It has been written to fulfil the graduation requirements of the Master's Programme in Science and Engineering at Tampere University.

The topic was selected based on my dream to one day become an expert in medical physics. This multidisciplinary work was related to medical physics, nuclear medicine, and meteorology, and rather than prior knowledge of the subject, the thinking learned during my studies in various problem-solving situations became the most important. During this endeavour, I also realised that struggling is often the key behind successful scientific process. Therefore, this project taught me precious lessons both professionally and personally.

I could not have undertaken this journey without the invaluable guidance and support my supervisors offered me. Words cannot express my gratitude to my academic supervisor, Professor Michiel Postema, for sharing his incredible expertise and for enriching my thinking, but also for helping me to plan the future of my scientific career. I would like to express my deepest appreciation to my daily supervisor, Medical Physicist Pasi Korkola from Tampere University Hospital, who was always ready to help, and with whom we had countless interesting conversations on the subject. He also introduced me to the hospital environment and the work of a medical physicist. I would like to extend my sincere thanks to Chief Medical Physicist Mika Kapanen from Tampere University Hospital for helping me to find this great topic which corresponded perfectly to my interest in medical physics.

Thank you to my family and friends for understanding and supporting me along the way. And finally, thank you, my reader: I hope you enjoy your reading.

Tampere, October 31, 2022

Nina Terho

Contents

List of Figures

List of Tables

List of Symbols and Abbreviations

Symbols

a	Inhaled activity	Bq
a, b, c, d	Dispersion coefficients	
C	Radioactivity concentration	$\mathrm{Bq/m^3}$
C/Q	Fall-out	$(\mathrm{Bq/m^3})/(\mathrm{Bq/s})$
$C_{\mathrm{corrected}}$	Concentration corrected for radioactive decay	$\mathrm{Bq/m^3}$
D	Total dose	Sv
D_{e}	External dose	Sv
D_{i}	Internal dose	Sv
D_{s}	Stack inside diameter	m
DC_{air}	Radionuclide-specific dose-rate factor for external irradiation	$(\mathrm{Sv/d})/(\mathrm{Bq/m^3})$
F	Buoyancy parameter	$\mathrm{m^4/s^3}$
g	Gravitational acceleration	$\mathrm{m/s^2}$
h	Physical source height	m
h_{eff}	Effective release height	m
h_{i}	Dose conversion factor for radionuclide i	Sv/Bq
Q	Material release rate	Bq/s
T	Ambient temperature	K
T_{s}	Stack gas temperature	K
t	Time elapsed after the release	s
t_{v}	Duration of the release	s

$t_{1/2}$	Half-life	s
u	Mean wind speed	m/s
V	Ventilation volume	m^3/h
V_i	Inhaled air volume	m^3
V_s	Stack gas speed	m/s
x	Distance from the source in wind direction	m
x_{max}	Downwind distance for the maximum plume rise	m
y	Crosswind distance from the plume centreline	m
z	Height above the ground	m
Δh	Plume rise	m
Δt	Duration of the exposure	s
λ	Radionuclide-specific decay factor	1/s
$\sigma_x, \sigma_y, \sigma_z$	Axial, horizontal, vertical dispersion parameter	m

Abbreviations

CT	Computed Tomography
FDG	^{18}F-Fluorodeoxyglucose
PET	Positron Emission Tomography
SILAM	System for Integrated Modelling of Atmospheric Composition
STUK	Radiation and Nuclear Safety Authority (Finnish: Säteilyturvakeskus)
TAYS	Tampere University Hospital
TIUKU	Collaborative Emergency Management Tool (Finnish: Tilanne- ja uhkakuvajärjestelmä)
VALMA	Transportation and Dose Calculation Model
VTT	Technical Research Centre of Finland (Finnish: Teknologian tutkimuskeskus)

1 Introduction

The number of radiopharmaceutical production facilities has been estimated to be growing worldwide, as the use of positron emitting radionuclides in medical diagnostics is in continuous growth [1], [2]. It is planned to start a cyclotron operation for self-sufficient radiopharmaceutical production at Tampere University Hospital (Tays). Before starting the operation, the hospital is required to provide a set of emission calculations which show that placing a cyclotron in the area will not cause any radiation safety risk for the population, that is, the dose reference levels defined by a radiation safety authority are not exceeded in any situation. This dissertation was executed as an order to Tays and the work is related to the hospital's cyclotron project. The purpose of this dissertation was to provide a calculation tool which can be used for modelling gaseous radioactive material concentrations at desired point in space (xyz) after the material is released into the atmosphere. It was intended to model concentration distributions in different planes and to use the modelled concentrations for dose calculations at individual points.

Gaussian air dispersion models have been used for describing the atmospheric behaviour and spread of gaseous materials in several applications, e.g., regulative calculations related to emissions arising from a medical cyclotron, modelling severe accidents on nuclear power plants and sulphur dioxide emissions from different factories [3]–[5]. In Finland, there are some atmospheric dispersion modelling software available. They are integrated as an emergency management system TIUKU (Finnish: Tilanne- ja uhkakuvajärjestelmä), developed as a collaboration of Radiation and Nuclear Safety Authority (STUK, Finnish: Säteilyturvakeskus) and Finnish Meteorological Institute since 2006 [6]. TIUKU can be used for running and displaying dispersion model results and dose calculations, and the system utilizes a long-range dispersion model, System for Integrated Modelling of Atmospheric Composition (SILAM), which is run by Finnish Meteorological Institute's supercomputers. Separate software, VALMA, developed in Technical Research Centre of Finland (VTT, Finnish: Teknologian tutkimuskeskus) is used for dose assessment in TIUKU. The software are however intended for significantly larger scale than the one studied in this dissertation, and their application is mainly in emissions arising from nuclear power plants: They have been used for simulating possible emission situations in Loviisa and Olkiluoto nuclear power plants, for instance. Executing this project

was important, because a complete model to describe a release situation at Tays was not available. Therefore, it was necessary to develop a calculation tool which describes specifically the studied situation, cyclotron exhausts in Tampere. The prevalent weather conditions, nature of the emission and properties of the emission source and the environment had to be incorporated into the model.

Cyclotron is the most widely used type of particle accelerator for production of radionuclides for medical applications, for example, positron emission tomography (PET) imaging [7]. Cyclotron consists of two D-shaped electrodes located between electromagnetic poles. An ion source, used to generate the charged particles is located near the centre of the electrodes. Voltage between the electrodes generates an electric field with a periodically altering direction. Inside the electrodes there is only a magnetic field generated by the electromagnet. The electrodes, electromagnet, and ion source are all contained in a vacuum. During the operation, the charged particles to be accelerated are directed to the cyclotron centre. The magnetic field inside the electrode causes the particles to move along a circular orbit. The particle moves a semicircle path inside the electrode, after which it returns to the electric field between the electrodes where its speed increases until it hits the other electrode and ends up to a circular orbit again. Deflection plate is used for bending the particle radius, enabling the particle beam to move through a window and collide with a target material. When the beam hits atom nuclei of the target, unstable radionuclides are produced. A schematic sketch, presenting two views, top (a) and side (b) of a cyclotron, is presented in Figure 1.

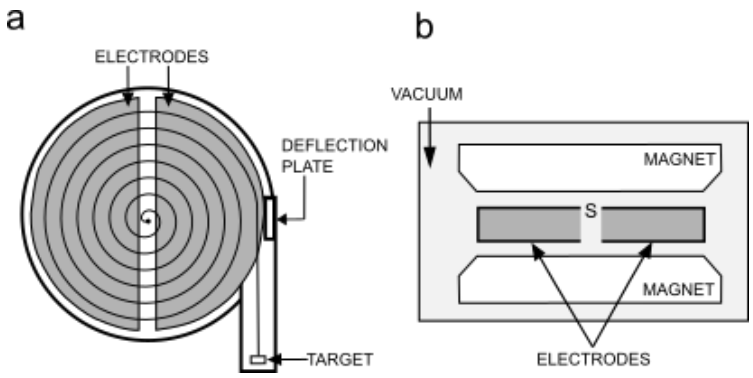

Figure 1. Two different views of a cyclotron. Top view is presented by a, side view by b. The letter S between the electrodes represents the ion source. Modified from [8].

Generally, radionuclides do not have many biologically interesting properties as

such. Therefore, radionuclides are attached as a label to a compound with interesting or useful biomedical properties to produce a radiopharmaceutical. Tracers labelled with radionuclides, radiopharmaceuticals, are used in nuclear medicine to direct radioactive material into a patient's body to a location to be treated or diagnosed. PET is a continuously increasing diagnostic technique and an important application of radiopharmaceuticals [9]. PET is based on the detection of two 511 keV annihilation photons originating from a positron-emitting source, e.g., a patient containing positron-emitting radioactivity. The radioactive material is guided to the patient body through e.g., injection. [8] Annihilation photons are emitted in opposite directions (180°) and they are detected nearly simultaneously, allowing to localize their origin along a line between two detectors. After the detector, photons are converted into electric signals by a photomultiplier tube. The electric signal is further processed by a computer to provide a three-dimensional image. Tays uses PET/CT machine which combines functional PET images with anatomical computed tomography (CT) images for more accurate diagnosis of diseases. In such machine, both scanners are mounted on a common gantry, PET unit in the back of the CT, attached to it.

Radioisotopes produced by a cyclotron are attractive for PET studies because of their high particle emission rations obtained in positron and electron capture decay. Fluorine-18 (^{18}F), which is produced in the form of a water solution, is a common cyclotron-produced radioisotope used in nuclear medicine, and it has a half-life $t_{1/2}$ = 109.8 min. ^{18}F is one of the most popular short-lived positron-emitting radionuclides and it is of great importance in the use as a label for PET radiotracers [10], [11]. One main application of ^{18}F is in the labelling of a glucose analogue, ^{18}F-fluorodeoxyglucose (FDG), which provides a measure of the metabolic rate for glucose in the cells of the body [8]. Due to a wide range of clinical applications, heart, brain, cancer [12], [13], FDG is the most widely used positron-emitting radiopharmaceutical [2], [8]. ^{11}C is the most stable artificial radioactive isotope of carbon, and it decays mainly due to positron emission, making it suitable for radioactive labelling of molecules in PET [14]. Relatively short half-life of ^{11}C, which enables consecutive studies in the same individual on the same day, is however long enough for multistep radiopharmaceutical synthesis. Compared to ^{18}F, lower radiation dose to the patient is resulted from the use of ^{11}C, and its radiochemistry options are less limited as no endogenous substance contain fluorine. [15] Other interesting short-lived radionuclides in relation to synthesis of endogenous compounds as PET tracers are oxygen-15 (^{15}O) and nitrogen-13 (^{13}N) which are used, for example, in patient

blood flow studies [16], [17]. ^{15}O has a half-life $t_{1/2}$ = 2.04 min, and it is used as a radioactive tracer in a form of ^{15}O water, a radioactive variation of regular water, in which the oxygen atom has been replaced by ^{15}O. The half-life of ^{13}N is 9.97 min.

FDG can be produced in regional distribution centres and shipped to hospitals located around hundreds of kilometres away because of the longer half-life of ^{18}F. Radiopharmaceuticals used at Tays are provided from a commercial supplier (MAP Medical Technologies OY/Curium) in Helsinki, for instance. However, because of significantly shorter half-life of ^{11}C, ^{15}O and ^{13}N, these isotopes require production on site with a dedicated biomedical cyclotron and rapid synthesis techniques to incorporate them into radiopharmaceuticals. Therefore, to enable the use of short-lived radionuclides, self-sufficient radiopharmaceutical production should be started by acquiring an own cyclotron in hospital campus area. Those short-lived nuclides are important from the medical point of view because their use would enable the production of clinically necessary radiopharmaceuticals, making PET imaging less limited. This would also make finding the correct diagnosis easier which is important also from the financial aspect as late diagnosis often leads to expenses for the treatment unit and it is also harmful for the patient [18]. The amount of PET studies has increased continuously for the last decade, mainly because of more accurate and sensitive imaging techniques and aging of the population [19]–[22]. With the increasing amount of imaging studies, the costs from buying radiopharmaceuticals constitute a significant expenditure for the treating unit. These aspects make self-sufficient and versatile radiopharmaceutical production essential for the clinical use. [23]

Producing and handling of radioactive materials are always related to radiation safety aspect. For radiation protection, cyclotron must be placed into a closed space with concrete walls of certain thickness. Also, because cyclotron products are usually further processed to make radiopharmaceuticals, premises for clean room operation are required. Cyclotron operation and radiopharmaceutical synthesis always generate radioactive waste which must be disposed. Different disposal methods exist depending on the type of waste, e.g., state of matter or amount, but for short-lived radionuclides produced by a medical cyclotron, the disposal method is usually an atmospheric release of the gaseous waste through an exit channel and the chimney of the accelerator laboratory. Therefore, an exhaust chimney must be placed in the vicinity of cyclotron laboratory. Radionuclides are always released into the atmosphere during chemical synthesis of radiopharmaceuticals, but in the case of target malfunc-

tion or failure, a large amount of activity may be released during short time-interval [3], [24].

After the release, the radioactive material travels and spreads in the atmosphere. Eventually, the material may enter to the human body and cause some serious tissue damage by irradiating there. In Finland, STUK is a government agency responsible for nuclear safety and radiation monitoring. STUK sets the regulations concerning emissions and waste resulting from the use of unsealed radioactive materials. According to STUK, the radiation dose of representative person, an individual receiving a dose that is representative of the most highly exposed individuals in the population, resulting from such operation must not exceed 10 μSv per year [25]. The operator must be able to show that this threshold value is not exceeded under any circumstances.

Several processes affect the transport of airborne radionuclides or any gaseous material. Advection is the movement of radionuclides along the prevalent wind field, i.e., downwind transport. The concentration of the material when it reaches some receptor point depends on the amount of dispersion of the material in the air. Dispersion results from some mixing processes, known as turbulent diffusion, which make the radioactive cloud to spread with respect to its centreline. Wet and dry deposition are processes which remove radioactive material from air to the ground. Rainout means that if the radionuclide becomes involved in precipitation formation processes within a cloud, the material is subsequently removed from the atmosphere with the precipitation. Washout refers to the material removal below a cloud by contact with falling precipitation. When the material becomes to contact with the ground, vegetation, or other obstacles, it becomes removed by dry deposition. Radioactive material is also removed from the atmosphere by radioactive decay. Figure 2 shows these processes affecting the transport of radionuclides released into the atmosphere.

To find the concentrations at locations downwind of the release, a model that considers these processes is needed. Air dispersion modelling is generally used technique to evaluate whether a release of a gaseous material causes some problem, e.g., whether a material concentration at any location exceeds some acceptable level for that location [27]. Acceptable concentration refers to population radiation safety when considering radionuclide releases. Therefore, for example, if it is planned to start a new cyclotron operation, the effect of resulting exhaust gases on the radiation safety of the population in the area can be predicted using an atmospheric dispersion model.

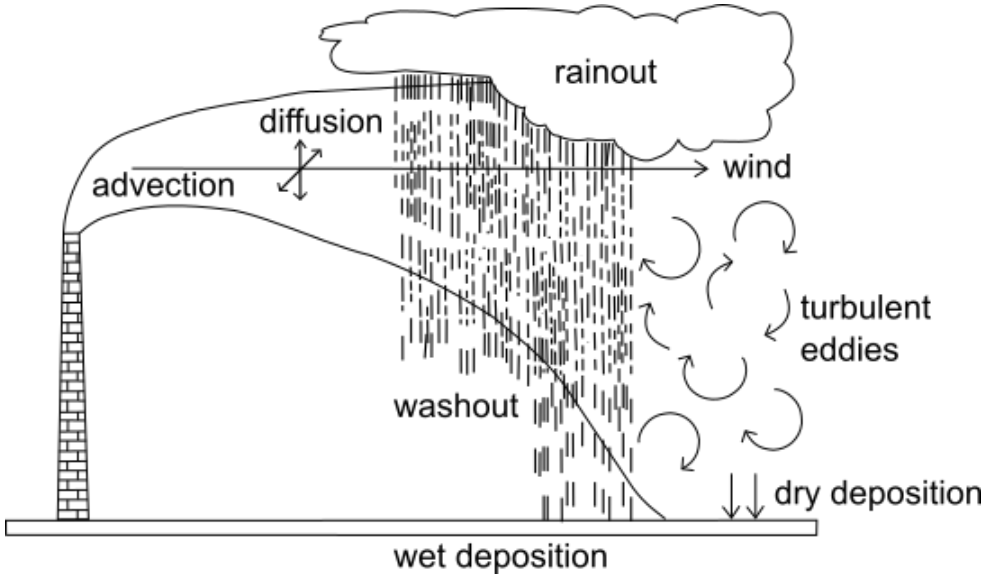

Figure 2. Processes affecting the radionuclide transport in the atmosphere. The material is transported downwind by advection. Diffusion caused by turbulent eddies makes the material spread from the cloud centreline. Wet and dry deposition remove the material from the air to the ground. Modified from [26].

A model suitable for the situation must be chosen based on nature of the release, terrain structure, prevalent weather conditions and the distance to be studied. As will be justified later, in this dissertation, we limit ourselves to study Gaussian models with certain prerequisites, assumptions, and limitations.

Two connected research questions were developed for this dissertation:

1. *How to model the dose of a representative person when radioactive materials are needed to be released into the atmosphere from a medical cyclotron in general case?*

2. *Based on the simulations, is it safe to build a medical cyclotron in Tays campus area?*

To answer the research questions, the following research objectives were determined:

1. *To apply a suitable spreading model to describe the radioactivity concentrations in the environment of the release. To use the maximum concentrations for calculating the total radiation dose of a representative person.*

2. *To calculate the maximum radiation doses resulting from the cyclotron operation at Tays and to compare the values to reference levels defined by an radiation safety authority.*

This dissertation is divided into six chapters. Chapter 1 introduces the research problem, providing motivation for the project, and gives an overview of the background of the study. The mathematics behind Gaussian dispersion models and dose calculations are introduced to the reader in Chapter 2. In Chapter 3, implementation of the work is described. An example code for concentration calculations is given in Appendix A. The most remarkable calculation results are presented in Chapter 4. All the obtained results are reported in Appendix B. Chapter 5 is dedicated for critically evaluating the dissertation outcome. The dissertation is concluded in Chapter 6.

2 Theory

This chapter focuses on the model and the mathematics behind the calculations of this dissertation. Gaussian dispersion models are generally used for describing the effect of wind on atmospheric pollutant concentrations. Gaussian model can be expressed in two ways, namely Gaussian puff model and Gaussian plume model. The puff model treats a continuous atmospheric release as a consecutive series of 'puffs' and describes the transport of each puff based on the source and wind field which can vary with space and time [28]. The model gives the instantaneous concentration from a single release, i.e., concentration as a function of time, C (Bq/m^3), as

$$C(x,y,z,t) = \frac{Q}{(2\pi)^{\frac{3}{2}}\sigma_x\sigma_y\sigma_z}\exp\left(-\frac{1}{2}\frac{(x-ut)^2}{\sigma_x^2}\right)\exp\left(-\frac{1}{2}\frac{y^2}{\sigma_y^2}\right) \left\{\exp\left[-\frac{1}{2}\frac{(z-h_{\text{eff}})^2}{\sigma_z^2}\right]+\exp\left[-\frac{1}{2}\frac{(z+h_{\text{eff}})^2}{\sigma_z^2}\right]\right\}, \quad (1)$$

where x, y, z are direction of the wind (x = 0 m at the source, $x > 0$ m downwind), horizontal direction perpendicular to the wind (y = 0 m at the plume centreline, $y >$ 0 m on the left from the centreline in the downwind direction), vertical direction (z = 0 m at the ground, $z > 0$ m above the ground) (m), respectively, t is time elapsed after the release, Q represents the material release rate (Bq/s), u is mean wind speed (m/s), $\sigma_x = \sigma_x(t), \sigma_y = \sigma_y(t), \sigma_z = \sigma_z(t)$ are time-dependent axial, horizontal and vertical dispersion parameters (m) and h_{eff} is the effective release height (m). The second exponential term within the curly brackets is the term due to assumed total material reflection at the ground. This means that the Gaussian models neglect the deposition processes removing the material from the atmosphere. At point (x, y, z) at time t, the total concentration is the sum of the concentrations of individual puffs.

Unlike plume model, puff model assumes dispersion also in x-direction as noted above. Hence, the model can produce accurate results also at low wind speeds ($u \ll$ 1 m/s) as it occasionally predicts pollution upwind, i.e., in the direction towards the source of the wind, when the dispersion is faster than the wind speed. Also, because the puff model gives the concentration as a function of time, it can be used to model situations when wind speed or direction is not constant over space or time.

Gaussian plume model is a simplification of the puff model. It describes a continuous release, a plume, which has a spread of Gaussian shape as it moves along

the wind. The model assumes constant, homogeneous turbulent flow, constant wind speed and direction and source release rate, resulting to a Gaussian concentration profile in lateral (y) and vertical (z) directions. In the wind direction (x), the dispersion is considered negligible compared to the downwind transport due to advection. The difference between the Gaussian plume and puff models is illustrated in Figure 3.

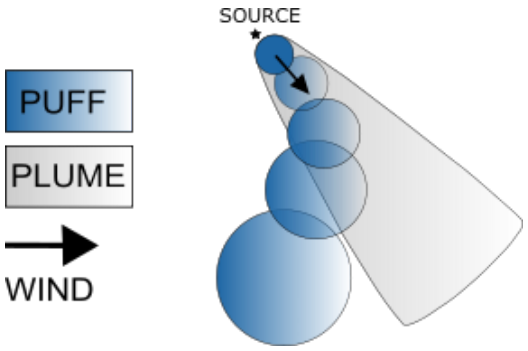

Figure 3. Schematic representation of the difference between plume and puff models. Both models are based on Gaussian shaped dispersion, but the puff model considers temporal and spatial changes in meteorological conditions. Modified from [29].

Assuming meteorological and source conditions constant in time is rarely true in the real atmosphere, so basically the assumption means that the plume travels from point A to B instantaneously. Therefore, the model can give reliable results only at relatively short distances, around $x < 10$–20 km. The model reliability increases along the use of empirical correlations for estimating the model parameters [27] . As it will be shown later in this chapter, Gaussian plume model considers several factors that influence the behaviour of a released plume: wind speed, atmospheric stability, plume temperature and gas exit speed. However, the model does not consider landscape or obstacles near the source of emission, making it inaccurate for situations where the terrain around the source is complex.

Gaussian plume model gives the time-independent material concentration C (Bq/m^3) as

$$C(x,y,z) = \frac{Q}{2\pi u \sigma_y \sigma_z} \exp\left(-\frac{1}{2}\frac{y^2}{\sigma_y^2}\right)\left\{\exp\left[-\frac{1}{2}\frac{(z-h_{\text{eff}})^2}{\sigma_z^2}\right] + \exp\left[-\frac{1}{2}\frac{(z+h_{\text{eff}})^2}{\sigma_z^2}\right]\right\}, \tag{2}$$

where x, y, z, Q, u and h_{eff} are defined as in Equation (1), and σ_y, σ_z are time-independent horizontal and vertical dispersion parameters (m). Due to the inverse

wind speed dependence of the equation, the inaccuracy of the plume models increases with u $\ll$ 1 m/s. Therefore, only wind speeds greater than that can be studied with Gaussian plume model. Radioactive fall-out C/Q ((Bq/m^3)/(Bq/s)) is obtained by dividing the Equation (2) by the radionuclide release rate.

Derivation of the Gaussian dispersion equations is beyond the scope of this dissertation. The reader interested in step-by-step derivation of the equations, considering all the theoretical prerequisites, assumptions and boundary conditions, is referred to the cited references [27], [30], [31]. As will be shown later, Gaussian plume model was used as a basis for the calculations of this dissertation. Hence, from now on, only the plume model is studied here. That is, the concentration given by the model becomes independent on time, and the plume dispersion in x direction is neglected.

If the prerequisites included in the plume model are not fulfilled in the studied situation, more advanced model is required. If e.g., the source or meteorological conditions cannot be assumed constant, the Gaussian puff model may be an appropriate choice. Further guidelines for choosing the model most appropriate for the situation are given in literature [28].

Concentration corrected for radioactive decay, $C_{\text{corrected}}$ (Bq/m^3), is obtained by multiplying the concentration given by the Gaussian plume equation (2) by a decay factor as

$$C_{\text{corrected}} = C \exp(-\lambda t), \tag{3}$$

where λ is radionuclide-specific decay constant (1/s) and t is the time elapsed after the release (s). Using the natural logarithm, the relationship

$$t_{1/2} = \frac{\ln 2}{\lambda}, \tag{4}$$

between λ and half-life, $t_{1/2}$ (s), is found. To eliminate time dependence of the concentration, t is expressed as a fraction of downwind distance x and mean wind speed u as

$$t = \frac{x}{u}. \tag{5}$$

Dispersion parameters, σ_y and σ_z, describe spread of the plume from the x-axis and hence give the profile shapes in each direction. They are defined through Briggs sigma curves [32] as

$$\sigma_y = ax^b$$
$$\sigma_z = cx^d\,, \tag{6}$$

where *a, b, c, d* are dispersion coefficients, constants depending on the atmospheric stability and the characteristics of source and surface. As measurements of atmospheric turbulence are not generally available, the atmospheric stability classification proposed by Pasquill, Gifford and Turner [33]–[36] is used for acquiring knowledge about the weather at the site of the emission. Stability class refers to a tendency for vertical mixing in the atmosphere, and it depends on the wind speed and the level of insolation in the daytime or cloudiness in the night-time. In this scheme, atmospheric stability conditions have been divided into six classes, A–F, corresponding to unstable, moderately stable, slightly unstable, neutral, slightly stable, and stable, respectively. Different sets for dispersion coefficients based on source and surface types have been developed [37]–[39]. The most suitable choice of coefficients for the situation depends on the source height, area type (urban/rural), and surface roughness.

When a plume is released from a chimney, it can rise from two reasons: 1) buoyancy due to high temperature of the gas or 2) momentum which is related to high exit velocity of the gas. Because the momentum contribution to the plume rise is usually small, it can often be neglected. Buoyancy again is the result of temperature difference between the gas and its environment. Effective release height h_{eff} (m) appearing in Equation (2) is due to initial plume buoyancy and it is calculated as

$$h_{\mathrm{eff}} = h + \Delta h, \tag{7}$$

where h is the physical stack height (m) and Δh is the plume rise (m). Several equations have been proposed for plume rise calculations, but the predictions of the different models differ more than factor of 10 from each other [40]. G.A. Briggs developed the most well-conceived equations for calculating the plume rise, and they are used in many regulatory models [41]. Next, Briggs algorithm [40], [42], [43] is applied for calculating Δh. The buoyancy parameter is calculated similarly for each stability class, but otherwise the procedure for calculating Δh is different depending on the stability conditions. The buoyancy parameter F ($\mathrm{m}^4/\mathrm{s}^3$) is calculated as

$$F = \frac{g}{4}\, V_{\mathrm{s}}\, {D_{\mathrm{s}}}^2\, \frac{T_{\mathrm{s}} - T}{T_{\mathrm{s}}}, \tag{8}$$

where $g = 9.81$ m/s^2 is the gravitational acceleration, D_s is the stack inside diameter (m), V_s is the stack gas speed (m/s), T_s is the stack gas temperature (K), and T is the ambient temperature (K). Depending on the value of F, the downwind distance at which the plume rise reaches its maximum x_{max} (m) is calculated as [40]

$$\begin{aligned} x_{max}(F < 55) &= 49F^{5/8} \\ x_{max}(F \geq 55) &= 119F^{2/5}, \end{aligned} \tag{9}$$

until $x < x_{max}$ the plume rise is calculated as [44]

$$\Delta h = \frac{1.6\ F^{1/3}\ x^{2/3}}{u}, \tag{10}$$

and it depends on the downwind distance of observation. After x_{max}, the plume rise remains constant and is calculated as

$$\Delta h = \frac{1.6\ F^{1/3}\ {x_{max}}^{2/3}}{u}. \tag{11}$$

For stable conditions, the equation for plume rise would be different, but as will be shown in Chapter 3, stable conditions are not studied in this dissertation.

Internal and external radiation doses are measures of radiation exposure in population. Internal dose D_i (Sv) means the radiation dose caused by radionuclides inside the body and it is calculated as

$$D_i = a \times h_i, \tag{12}$$

where a is the amount of inhaled activity (Bq) and h_i is the dose conversion factor for radionuclide i (Sv/Bq). Radioactive materials may enter to the body via inhalation or food intake. Inhaled activity at an individual point (x, y, z) is calculated using the radioactivity concentration obtained from the Gaussian equation as

$$a = C \times V_i, \tag{13}$$

where V_i is the inhaled air volume (m^3), determined using the ventilation volume V (m^3/h) and duration of the exposure Δt (s) as

$$V_i = \Delta t \times V. \tag{14}$$

When the maximum concentration lies at the midpoint of emission drift, duration of the exposure is evaluated as

$$\Delta t = t_v + \frac{x/u}{2}, \tag{15}$$

where t_v is duration of the release (s).

External dose is directed to a human from radiation sources outside the body. At an individual point (x, y, z), external dose, D_e (Sv), is calculated using the radioactivity concentration obtained from the Gaussian equation as

$$D_e = DC_{air} \times C, \tag{16}$$

where DC_{air} is the radionuclide-specific dose-rate factor for external irradiation ((Sv/d)/(Bq/m^3)). The total dose, D (Sv), determined as the sum of internal and external dose as

$$D = D_i + D_e \tag{17}$$

is used as a measure when the amount of radiation exposure is compared to the dose limits given by STUK.

3 Methods

In this dissertation, two release scenarios were modelled: a) Accidental leak, where a large amount of radioactive material is released into the atmosphere during short time interval, b) Continuous, small release caused by a normal use of cyclotron. The cyclotron-produced radioisotopes chosen for modelling were ^{18}F and ^{11}C. Radioactive fall-out and concentration of ^{18}F and ^{11}C were modelled in different planes. Based on the modelled concentrations, radiation doses were calculated. Scenario a) was modelled only with ^{11}C, and b) with both ^{11}C and ^{18}F.

The choice of an appropriate dispersion model was made by comparing the situation to be studied to the assumptions, prerequisites, and limitations of different models. Release rate Q and wind speed u were assumed to be constant and non-zero in the modelled situation. Wet and dry deposition processes were neglected. Gaussian plume model, presented in Equation (2), was chosen for concentration calculations. Concentration given by the plume model was corrected for radioactive decay by using Equation (3).

Wind roses describing the wind statistics at two measurement stations at Tampere were obtained from Finnish Meteorological Institute. The average value of u was used as an input parameter in Equation (3). The wind roses are presented and interpreted in Appendix A.1. Stability class corresponding to the situation was found after studying solar elevation angles at Tampere. At Tampere, the angle is never over 60° above the horizon. It was found that around noon, the angle lies between 35–60° for 5 months per year and 15–35° for 4 months per year. The angle is under 15° for 3 months per year. Based on the mean wind speed and solar elevation angles, the stability class corresponding the situation was found to be C, slightly unstable.

After determining the stability class, values for the constants a–d appearing in Equation (6) were chosen. The constants determined for a situation with high stacks and for smooth to medium rough surfaces [38] were chosen for the calculations.

Values for h, V_s, D_s, T_s and T were evaluated and chosen after consulting medical physicist Pasi Korkola (Tays). For T_s and T, room temperature and annual average temperature at Tampere, respectively, were used.

The release rate values were chosen after consulting Chemist Semi Helin (Turku PET Centre / Tays). It was decided to use the Q values that have been realised at Turku PET Centre from similar cyclotron operation. For continuous, normal release, the

released activities were 350 GBq/a, and 120 GBq/a with ^{11}C and ^{18}F, respectively. In accidental leak, 350 GBq activity of ^{11}C was released. To find the release rates, the usage of cyclotron and the duration of the release were evaluated. With the assumption of 240 operation days and the synthesis duration of 60 min, the annual release rates, corresponding to normal release, of 24.3 MBq/s (^{11}C) and 8.3 MBq/s (^{18}F) were found. ^{11}C release rate in accident situation, 5.8 GBq/s, was found by dividing the total released activity by the duration of the release, which was expected to be 60 s. The step-by-step solution for calculating the release rates from the released activities is presented in Appendix A.2.

Gaussian plume equation was always applied with the following input parameters: u = 4 m/s, V_s = 4 m/s, D_s = 0.8 m, T_s = 293.15 K and T = 277.55 K, h = 30 m, a = 0.36, b = 0.86, *0.33*, and d = 0.86. Modelling was performed in MATLAB® (The MathWorks, Inc., Natick, MA, USA) environment.

The first phase of modelling was to study the radioactive fall-out. The ground level fall-out curve of ^{11}C and ^{18}F was drawn in the same figure. The values for u , V_s, D_s, T_s, T, h, a, b, c, and d were substituted in Equation (3). The fall-out was modelled as a function of x from 0 to 300 m with 0.1 m intervals downwind (y = 0) from the source. Effective height was calculated using Equations (7)–(11). Correction for radioactive decay for each isotope was performed using Equations (3)–(4). Fall-out was obtained by dividing the concentrations of each isotope by the corresponding release rates. Fall-out curves and the point of maximum fall-out were drawn using *plot()* command.

^{11}C ground-level fall-out was modelled also with another two wind speeds, u_2 = 1.5 m/s and u_3 = 7.0 m/s. The procedure was like the one for drawing the ^{11}C and ^{18}F fall-out except for two steps. First, it was studied whether different wind speed leads to different stability class and constants appearing in Equation (6). It turned out that u_2 led to stability class B, moderately unstable, for which the constant values a–d were the same as for u = 4m/s. Stronger wind speed, u_3, corresponded to the stability class D, neutral, which led to different set of constants in Equation (6): a_3 = 0.32; b_3 = 0.78; c_3 = 0.22; d_3 = 0.78. Second, the downwind distance to be modelled was set to distances 0–400 m with 0.1 m intervals. The radiation doses were calculated at the ground-level points of maximum fall-out and concentration with u_2 and , u_3 using Equations (12)–(17).

Five different heights were chosen for the concentration distribution calculations: z = 0.0, 5.0, 10.0, 20.0 and 32.4 m. Height z = 0 described the ground-level and z = 32.4

was the effective release height obtained from equations (7)–(11). Heights 5.0, 10.0 and 20.0 demonstrated typical floor and building heights. Maximum concentrations in wind direction ($y = 0$) were found at those five heights. The maximum concentration and the distance at which it occurs was found by using command *[M,I] = max(c)*.

^{11}C concentrations in accidental leak at different xy combinations were calculated at five heights. Values appearing in Equation (3) were otherwise kept unchanged, but downwind distance was set to have values from 0 to 150 m with 10 m intervals. Concentrations were calculated by increasing y with 10 m intervals until the concentration was under 1‰ of the maximum value at the studied height. Concentrations over one thousandth of the maximum concentration at the height to be studied were written in Tables 3–7 presented in Appendix B.1. Smaller values were left out from the dose calculations.

Based on the calculated concentrations, the xyz-points for dose calculations were chosen. ^{11}C concentrations in normal release were calculated at the same points as in accidental leak. The effect of correction for the radioactive decay in Equation (3) was assumed to be small, and ^{18}F concentrations at different xy combinations were not studied as extensively as with ^{11}C. Y-values were iteratively chosen only at the downwind distances x, where the maximum concentration occurs at five heights. This led to 30 calculation points at which the concentration is over 1‰ of the maximum at each height. The concentration values were written in tables 11–13 presented in Appendix B.3.

Concentration profiles were drawn in accidental leak of ^{11}C. First, five xy concentration profiles of ^{11}C were drawn with z = 0.0, 5.0, 10.0, 20.0 and 32.4 m. All the constants in Equation (3) were kept unchanged. Distances x and y was chosen to range from 0 to 200 m and from -110 to 110 m with 0.1 m intervals, respectively. MATLAB® code for calculating concentrations and drawing concentration profiles is presented in Appendix A.3.

Two more concentration profiles of ^{11}C in accidental leak were drawn in xz plane. The first xz profile was drawn near the height of the release: z ranged from 30 to 36 m with 0.1 m intervals. The range for x was chosen to be 5–40 m with 0.1 m intervals. The second xz profile was drawn in larger scale: z = 0–60 m and x = 40–140 m with 0.1 m intervals in both x and z directions.

Radiation doses were calculated at above iteratively chosen points. At the level of effective release height, additional distances x were included into the calculations. Internal dose was calculated using Equations (12)–(15). Duration of release, t_v, in

Equation (15) was evaluated to be 1 min in accidental leak and 60 min in normal release. Ventilation volume in Equation (14) was evaluated to be 0.9 m^3/h, which is 1.5 times the rest ventilation volume of an adult [45], [46]. Values used for dose conversion factor in Equation (12) were 2.4×10^{-11} Sv/Bq (^{11}C) and 4.9×10^{-11} Sv/Bq (^{18}F) [47]. External dose was calculated using Equation (16) with dose-rate factor values 3.8×10^{-9} (Svd^{-1}/Bqm^{-3}) for ^{11}C and 3.7×10^{-9} for ^{18}F [48]. Finally, the total dose at each point was calculated along Equation (17). The procedure was repeated for each three situations: accidental leak of ^{11}C, normal release of ^{11}C and normal release of ^{18}F. Finally, the results were compared to the maximum allowed dose, 10μSv, resulting from this kind of operation.

4 Results

This chapter focuses on presenting the most remarkable calculation results of this dissertation. Additional results are included in Appendix B.

Maximum concentrations of ^{11}C and ^{18}F were found at five different heights. Table 1 shows ^{11}C concentrations (Bq/m^3) and the corresponding radiation doses (μSv, μSv/a) at the downwind distances x where the maximum concentration was met at each height in accidental leak and normal release. Maximum ^{18}F concentrations (Bq/m^3) and the corresponding doses (μSv/a) are shown in Table 2. From Tables 1–2, it can be seen that as the point of observation moved higher, i.e., z approached the effective release height, the value of maximum concentration increased and moved closer to the source. In each situation, the dose value exceeded 10 μSv at $z = h_{\text{eff}}$. In Appendix B.1, ^{11}C concentration values in accidental leak are presented with five different z values and several xy combinations. The tables show how far from the plume centreline concentrations greater than 1‰ of the maximum occurred. All the calculated concentrations, the corresponding doses and the intermediate results of the dose calculations are presented in Appendices B.2–B.3.

Table 1. ^{11}C maximum concentrations (Bq/m^3) at five different heights and the resulting radiation doses of the representative person in accidental leak and normal release. While the dose resulting from accidental leak is instantaneous (μSv), normal release leads to annual dose (μSv/a). As z approached h_{eff}, the values of maximum concentration and dose increased and the distance of the maximum, x, moved towards the source.

	Concentration (Bq/m^3)		Dose (μSv)	Dose (μSv/a)
x, y, z (m)	Accident	Normal	Accident	Normal
(137.4, 0.0, 0.0)	1.5×10^5	611.0	0.57	0.11
(113.2, 0.0, 5.0)	2.1×10^5	857.8	0.76	0.15
(89.6, 0.0, 10.0)	3.1×10^5	1.3×10^3	1.1	0.23
(45.1, 0.0, 20.0)	1.0×10^6	4.2×10^3	3.3	0.77
(5.0, 0.0, 32.4)	6.1×10^7	2.6×10^5	190	46

Figure 4 shows the ground-level fall-out, C/Q ((Bq/m^3)/(Bq/s)), of ^{11}C and ^{18}F as a function of downwind distance, x, which ranges from 0 to 300 m with 0.1 m

Table 2. ^{18}F maximum concentrations (Bq/m^3) at five different heights and the resulting annual radiation doses of the representative person (μSv/a) in normal release. As z approached h_{eff}, the values of maximum concentration and dose increased and the distance of the maximum, x, moved towards the source.

x, y, z (m)	Concentration (Bq/m^3)	Dose (μSv/a)
138.2,0,0	212.9	0.042
113.7,0,5.0	298.0	0.059
89.9,0,10.0	446.5	0.089
45.2,0,20.0	1.5×10^3	0.29
5.0,0,32.4	8.8×10^4	18

intervals. The red dots in the curves represent the point x where the fall-out reached its maximum. With ^{11}C (yellow curve), the maximum fall-out value of 2.5 $\times10^{-5}$ (Bq/m^3)/(Bq/s) was met at 137.4 m from the source. With ^{18}F (blue curve), the maximum fall-out value of 2.6 $\times10^{-5}$ (Bq/m^3)/(Bq/s) was met at 138.2 m from the source.

Figure 5 shows the ground level (z = 0) ^{11}C fall-out, C/Q ((Bq/m^3)/(Bq/s)), as a function of downwind distance x with three different wind speeds: 1.5, 4.0 and 7.0 m/s. The x-axis values range from 0 to 400 m with 0.1 m intervals. The red dots in the curves represent the point x where fall-out reached its maximum. Green curve corresponds to wind speed of 1.5 m/s which results in the greatest fall-out value, 6.5 $\times10^{-5}$ (Bq/m^3)/(Bq/s). Also, with this wind speed, the maximum fall-out value was met closest to the source, at x = 136.0 m. Blue and yellow curve represent the wind speeds of 4.0 and 7.0 m/s, respectively. Wind speed of 4 m/s led to maximum fall-out of 2.5 $\times10^{-5}$ (Bq/m^3)/(Bq/s) 137.4 m away from the source. With wind speed of 7.0 m/s, the maximum fall-out of 1.1×10^{-5} (Bq/m^3)/(Bq/s) was met 380.1 m away from the source. With the used u values, all the fall-out maximum values were of the same order of magnitude. As shown in Table 1, when u = 4 m/s, the maximum dose was 0.57 μSv in accidental leak of ^{11}C. When the wind speed was 7 m/s, the maximum dose decreased to 0.27 μSv. The lower wind speed, 1.5 m/s, led to the greatest maximum dose, 2.0 μSv.

^{11}C concentration profiles at heights z = 0.0, 5.0, 10.0, 20.0 and h_{eff} = 32.0 m (a–e) in accidental leak are presented in Figure 6. Downwind distance x ranges from

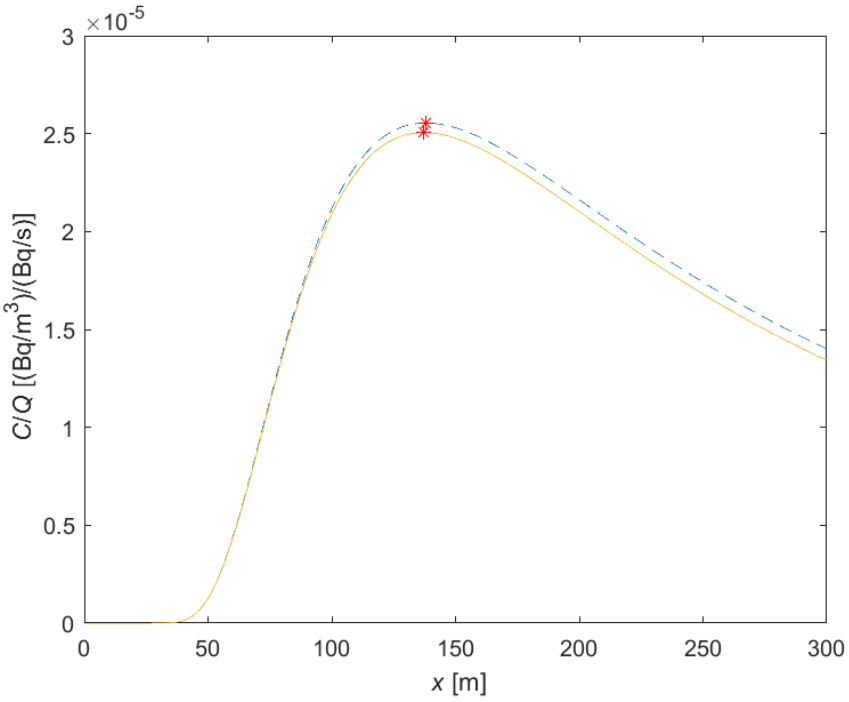

Figure 4. Ground-level (z = 0) fall-out C/Q ((Bq/m^3)/(Bq/s)) as a function of downwind distance x (m). The range of x-axis is 0–300 m with 0.1 m intervals. Yellow curve describes the fall-out of ^{11}C, blue is for ^{18}F. The red dots represent the point of maximum fall-out for each isotope: $(C/Q)_{max,^{11}C}$ = 2.5 ×10^{-5} (Bq/m^3)/(Bq/s) at x = 137.4 m and $(C/Q)_{max,^{18}F}$ = 2.6 ×10^{-5} (Bq/m^3)/(Bq/s) at x = 138.2 m.

40 to 200 m with 0.1 m intervals. The range for crosswind distance y is -110–110 m with 0.1 m intervals. The colorbar on the left of the map a describes the concentration range (Bq/m^3) of each color as follows: yellow: > 10^5, lighter blue: 10^4–10^5, darker blue: 10^3–10^4 and white: < 10^3. The figure demonstrates that as z increased, the point of maximum concentration moved towards the source. Larger concentrations were also met on a broader area with increased z values.

Figure 7 demonstrates xz concentration profile of ^{11}C downwind (y = 0 m) from the source in accidental leak. The range in vertical direction is 30–36 m with 0.1 m intervals, so the z values are close to the effective release height h_{eff}. X-axis values range from 5 to 40 m with 0.1 m intervals. The colorbar describes the concentrations (Bq/m^3) corresponding different (xz) points. Yellow is for the greatest concentrations, ≥ 12×10 ^{7} (Bq/m^3). The darkest blue represent the smallest concentrations, < 2×10^7 (Bq/m^3). The figure shows that near the level of release the maximum concentration occurred 0–5 m away from the source and after that the concentration diluted in the

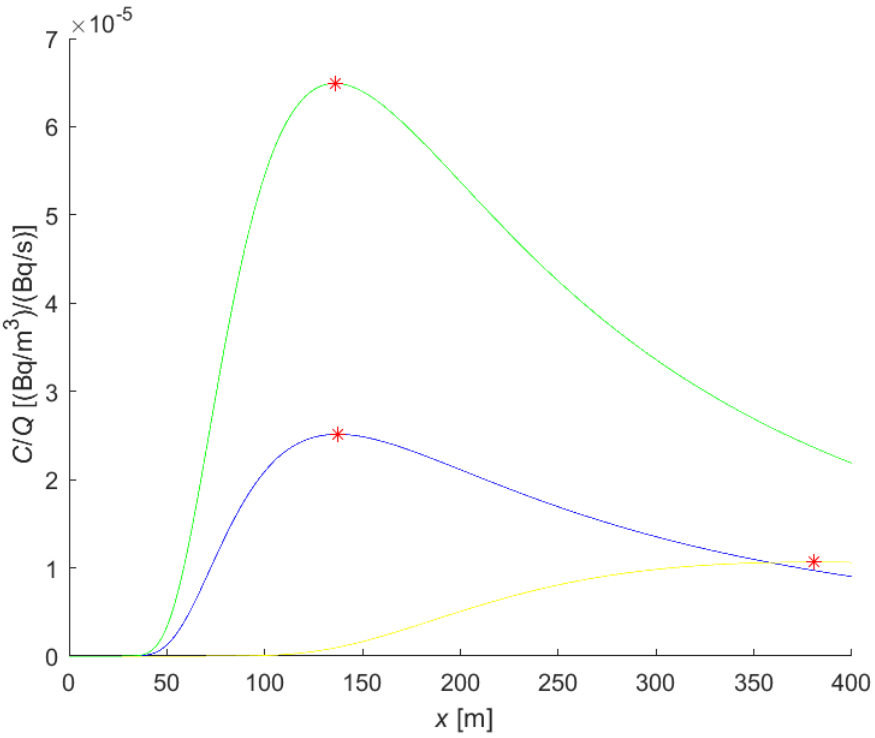

Figure 5. Ground-level fall-out C/Q ((Bq/m^3)/(Bq/s)) of ^{11}C as a function of downwind distance x (m) with three different wind speeds. The range of x-axis is 0–400 m with 0.1 m intervals. Green curve corresponds to u = 1.5 m/s, blue for u = 4.0 m/s and yellow u = 7.0 m/s. The red dots represent the point of maximum fall-out with each value of u. With wind speed of 1.5 m/s, $(C/Q)_{max,1.5}$ = 6.5 ×10^{-5} (Bq/m^3)/(Bq/s) at x = 136.0 m. Wind speed of 4 and 7 m/s resulted in $(C/Q)_{max,4.0}$ = 2.5 ×10^{-5} (Bq/m^3)/(Bq/s) at x = 137.4 m and $(C/Q)_{max,7.0}$ = 1.1 ×10^{-5} (Bq/m^3)/(Bq/s) at x = 380.1 m.

surrounding air mass.

Figure shows the xz concentration profile of ^{11}C in accidental leak with wider x and z ranges than in Figure 7. Z-values vary from the ground level to 60 m with 0.1 m intervals. The range in x direction is 40–140 m with 0.1 m intervals. The colorbar describes the concentrations (Bq/m^3) corresponding different (xz) points. Yellow is for the greatest concentrations, ≥ 3×10 ^{6} (Bq/m^3). The darkest blue represents the smallest concentrations, < 0.5×10^6 (Bq/m^3). The figure shows that the greatest concentrations were met near the level of effective release height, at downwind distances x < 40 m, but concentrations of the order of 10^6 Bq/m^3 were met up to around 120 m away from the source.

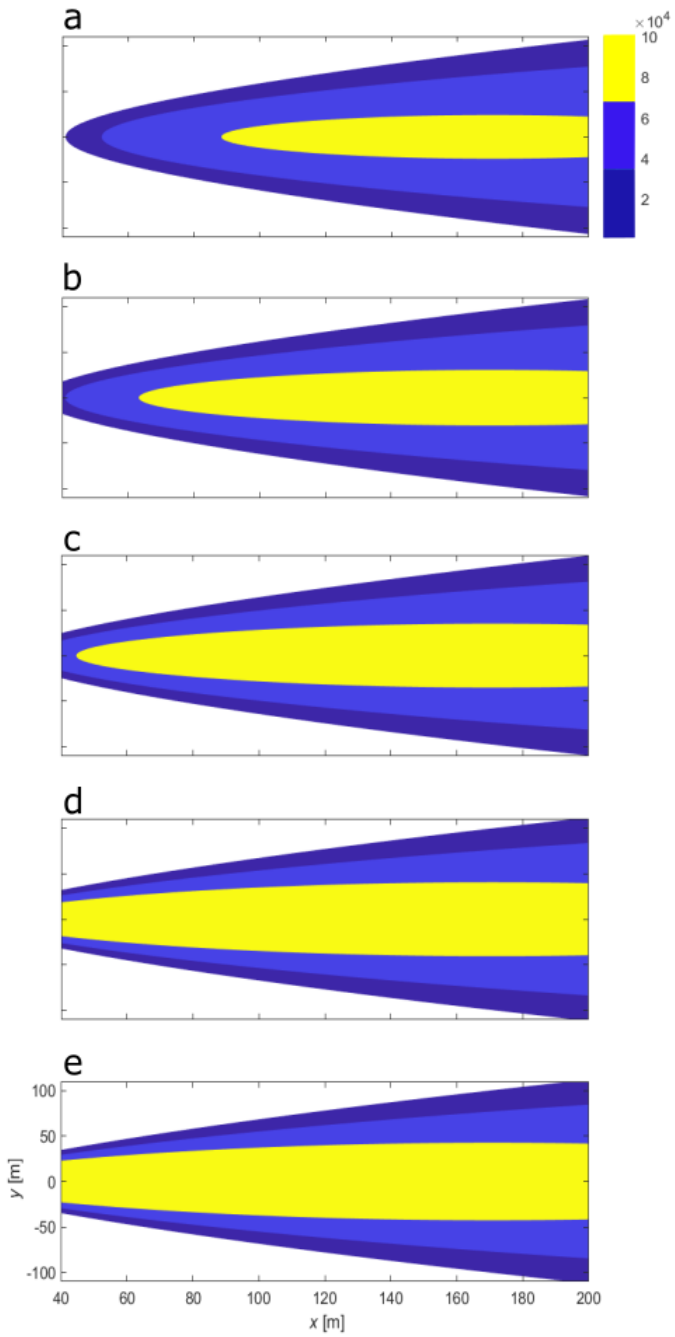

Figure 6. ^{11}C concentration profiles in accidental leak at heights z = 0.0, 5.0, 10.0, 20.0 and 32.0 m (a–e). Y- and x-axis values range from -100 to 100 m and 40 to 200 m with 0.1 m intervals, respectively. Colors represent the following concentration ranges: yellow > 10^5, lighter blue = 10^4–10^5, darker blue = 10^3–10^4 and white 0–10^3 Bq/m^3. Maximum concentration moved towards the source and increased with increasing z. Also, the area of larger concentrations broadened as z increased.

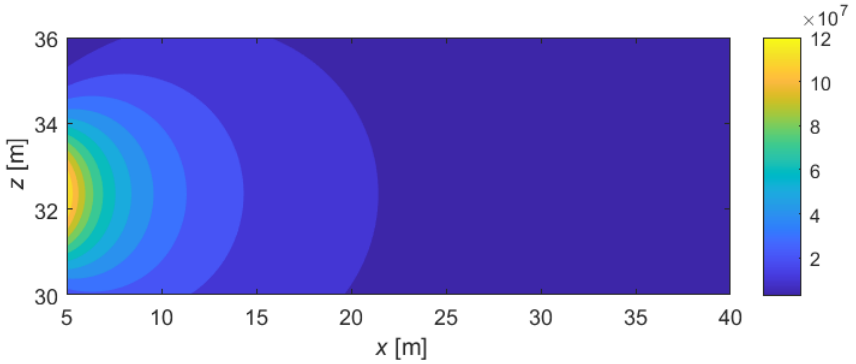

Figure 7. Downwind (y = 0) concentration profile of ^{11}C in accidental leak. Z-axis range: 30–36 m, x-axis range: 5–40 m, both with 0.1 m intervals. The colorbar describes the concentration values: yellow is for concentrations ≥ 12×10 ^{7} (Bq/m^3), the darkest blue for concentrations < 2×10^7 (Bq/m^3). The maximum concentration was found at the level of h_{eff}, at $x \leq 5$ m.

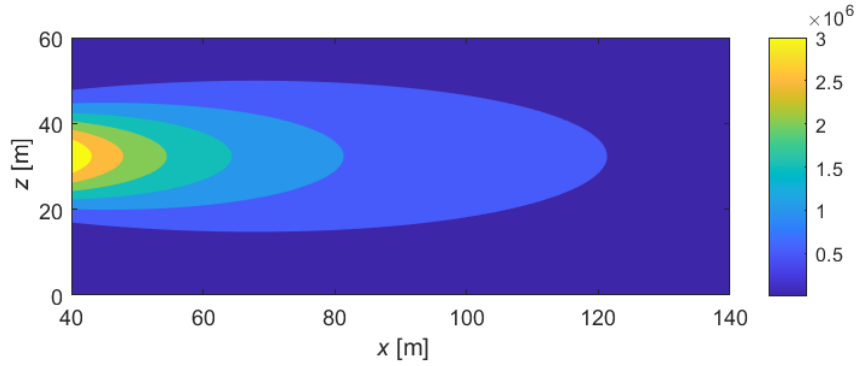

Figure 8. Downwind (y = 0) concentration profile of ^{11}C in accidental leak with z = 0–60 m and x = 40–140 m, both with 0.1 m intervals. The colorbar describes the concentration values: yellow is for concentrations ≥ 3×10 ^{6} (Bq/m^3), the darkest blue for concentrations < 0.5×10^6 (Bq/m^3). The maximum concentration was found at the level of h_{eff}, at x ≤ 40 m.

5 Discussion

The purpose of this dissertation was to provide and exploratory study of the spread of radioactive materials released into the atmosphere because of medical cyclotron operation and radiopharmaceutical production. It was intended to model the radioactivity concentrations and use the modelled concentrations for radiation dose calculations in a schematic situation where cyclotron operation for radiopharmaceutical production would be started at Tays. It was also anticipated that the provided calculation tool would be applicable not only in Tays case, but also universally. Therefore, the tool could be utilized and developed further for similar projects. This chapter focuses on having a critical look to the methodology of this dissertation. Reliability of the obtained results is evaluated, and it is also discussed, how representative the results are. The chapter ends with discussing the limitations of this study and providing recommendations for future research.

Two types of dispersion models, Gaussian puff and plume model, were introduced in Chapter 2. In this dissertation, Gaussian plume model was used for modelling the atmospheric radioactivity concentrations resulting from medical cyclotron operation. The plume model was chosen for the calculations after comparing the situation to be studied to the assumptions, prerequisites, and limitations of different models. For long transport distances, about $\gtrapprox$ 10–20 km from the source, the puff model would be more appropriate choice as wind speed and direction may change during the travel. Also, the influence of complex terrain on varying flow fields will increase along the transport distance. However, it was known that the area to be modelled consists of the hospital environment because 1) the intention was to find the maximum concentrations and 2) as the radioactive material is transported along the wind, the activity concentrations decrease as the material becomes removed from the atmosphere by radioactive decay. Therefore, the modelling could be limited to the near-field where reliable results can be obtained by a Gaussian plume model, which basically assumes instantaneous plume transport from point A to B. Wet and dry deposition could also be neglected because of the short half-lives of the studied radionuclides. The maximum concentration was needed to find at any point of time. Hence, the assumption of constant release rate and wind speed could be made to obtain time-independent material concentrations. Also, the prerequisite of non-zero wind speed in Equation (2) was fulfilled as the minimum wind speed found from wind statistics at Tampere

was 0.5 m/s. The used model is applicable for concentration calculations as such in unstable and neutral atmospheric stability conditions, corresponding to stability classes A–D. Applying the model for stable conditions (E–F) would require modifications in effective release height calculation procedure. The experimental constants determining dispersion coefficients were rather qualitatively chosen to correspond relatively high stacks and smooth to medium rough terrain [38]. The experimental constants determined for surface/low sources with rough surface and urban area by McElroy and Pooler [37] would have also been a possible choice. If the model was applied in environment different from Tays area, the constants most appropriate for the situation should be chosen by evaluating the terrain characteristics and nature of the emission source.

Gaussian plume model is a simplification of the puff model, and it enables faster and less complex calculations because of fewer number of variables resulting from the assumptions made concerning meteorological conditions and terrain properties. However, it cannot be claimed that the plume model would always be an appropriate choice for modelling the exhausts from a medical cyclotron, but the choice of model must always be done by precisely considering the situation to be studied. For example, in a situation of a complex terrain or on a coastal site, air pollution concentrations are commonly affected by terrain effects and highly variable airflows, and plume models, which assume constant meteorological conditions, may not provide the most reliable results.

Ground-level fall-out of ^{11}C and ^{18}F was presented as a function of downwind distance. The ground level fall-out curves of ^{11}C and ^{18}F were drawn in the same figure to find the effect of different radioactive decay factors. The maximum fall-out value differed by 0.1 (Bq/m^3)/(Bq/s). The downwind distance at which the maximum occurs differed by 0.8 m. The result gives a hint that if the half-lives of two isotopes are close to each other, the correction for radioactive decay in Equation (3) does not cause significant difference in the outcome. Actually, if the fall-out of an isotope with longer half-life, e.g., ^{137}Cs with $t_{1/2} \approx 30$ year or ^{90}Sr with $t_{1/2} \approx 29$ years, was drawn in the same figure, the curves would overlap with the ^{18}F curve. This is because with the half-lives of ^{18}F, ^{137}Cs and ^{90}Sr basically no radioactive material is removed from the atmosphere by radioactive decay before the plume reaches the point of maximum concentration by means of other processes affecting its transport. With ^{11}C, which has the shortest half-life of the four, again, at the downwind distance where the maximum occurs with the other three isotopes, some material is already

removed from the atmosphere by radioactive decay. Especially with all the other assumptions and simplifications made in the calculations, it would be justifiable to neglect the effect of radioactive decay.

The complete calculations in this dissertation were performed using only one value for wind speed. Wind statistics at two near-by measurement stations with respect to Tays were provided from Finnish Meteorological Institute. Neither of the measurement stations corresponded perfectly to the hospital campus area as Siilinkari is located on lake Näsijärvi and Tampere-Pirkkala airport is an open area without many obstacles surrounding it. Therefore, an average wind speed of the two, 4 m/s, was chosen for the calculations. Wind speed appears in Equation (2) as such, but the determination of dispersion parameters in Equation (6) also depends on it. Hence, the results do not apply as such in a situation where wind speed differs from the average value at the time of radioactivity release. Therefore, the impact of different wind speed on the resulting radioactivity fall-out was studied. It was proven that the maximum fall-out values corresponding to three different wind speeds had the same order of magnitude. As the fall-out decreases with increasing wind speed, also the radioactivity dose at the point of maximum concentration is smaller than the corresponding maximum concentration obtained in the calculations with 4 m/s wind speed. However, with smaller wind speed, the maximum fall-out and the resultant dose is greater than in the studied case. The maximum ground level doses with three different wind speed differed up to one order of magnitude. This may be noticeable in a situation where doses are near the acceptable limit already with the wind speed used for the complete calculations. One should however be aware of all the other assumptions and approximations made in the calculations which make the doses to be only estimates. The additional wind speeds were chosen to be significantly 1) smaller and 2) greater than the value used in complete calculations. These wind speeds and the mean solar elevation angles at Tampere led to stability classes B, moderately unstable, and D, neutral. Situations corresponding to stability classes E–F, slightly stable and moderately stable, were not considered in the calculations because they occur only during night-time, and the cyclotron is operating only during daytime. Except for the buoyancy parameter F, stable atmospheric conditions require different procedure for calculating effective release height and the outcome is therefore also different. Briggs method for calculating the effective height [44] is recommended to be studied if one needs to model concentrations under stable conditions.

To get an idea about concentration distributions at different heights with respect

to the source, five different heights were chosen for the calculations. To find out up to which distances y from the plume centreline significant concentrations occur, ^{11}C concentrations at different xy combinations were calculated at five heights. Concentrations under 1‰ of the maximum value at the studied height were not considered significant and were left out from the dose calculations. Similar concentration calculations were performed also for normal release of ^{11}C and ^{18}F, but because the effect of correction for the radioactive decay in Equation (3) could be assumed to be small, ^{18}F concentrations at different xy combinations were not studied as extensively as with ^{11}C.

The modelled concentrations were used for individual point dose calculations in three schematic release situations at Tays: 1) accidental leak of ^{11}C, 2) normal release of ^{11}C and 3) normal release of ^{18}F. Radiation safety risk of the population in the environment of the hospital was evaluated based on calculated doses.

Concentration profiles were drawn only in one situation, accidental leak of ^{11}C, to demonstrate 1) the xy concentration distributions at different heights and 2) xz concentration distributions at the plume centreline. Concentration profiles gave an encompassing view, with 0.1 m accuracy, of how the consentration is distributed in different xy and xz planes. One remarkable assumption made in the calculations is flat terrain which means basically ground level being always at $z = 0$. This assumption is not very accurate because of terrestrial elevation. As the concentration values vary at different heights, the flat terrain assumption can cause significant errors in dose calculations. Around the planned cyclotron location at Tays, there are no major differences in elevation, but the assumption that the ground level at the point of observation is the same as at the point of release is not necessarily exactly true.

Dose calculations revealed that the maximum allowed dose of a representative person, 10 μSv, was exceeded in each three scenarios, accidental leak of ^{11}C, normal release of ^{11}C and normal release of ^{18}F at height 32.4 m, i.e., the effective release height. Hence, if the chimney height was increased enough, one could achieve a situation where the radiation dose would be negligible at the heights where people are staying on continuous basis. However, on Tays campus, the chimney height is limited because of the helicopter landing area located on the nearby building roof.

Accidental leak of ^{11}C led to 190 μSv instantaneous radiation dose. Normal release of ^{11}C and ^{18}F caused radiation doses of 46 and 18 μSv, respectively. ^{18}F release resulted in smaller annual dose compared to ^{11}C because of smaller amount of released activity. As stated before, cyclotron-produced ^{18}F is in a form of water

solution, and hence it cannot be assumed that the substance would instantaneously change from liquid to gas and all the produced activity could escape to the exit channel. Produced activity is therefore probably significantly greater than the amount released into the atmosphere, unlike with ^{11}C which is initially in gaseous state. In accidental leak, ^{11}C doses exceeded the 10 μSv dose limit up to 45 m away from the source. In normal release, the annual limit was exceeded up to 20 and 45 m with ^{11}C and ^{18}F, respectively. The result set up a restriction for placing any buildings of same height as the effective height within a 45 m radius from the source when terrestrial elevation is not considered. The maximum values do not lie in the acceptable range but are however small compared to possible doses resulting from ionising radiation, for example, the radiation dose received by a patient from a lung X-ray (0.1 mSv), the average annual radiation dose for Finns caused by indoor radon, X-ray examinations, etc. (5.9 mSv), or the dose which may cause symptoms of a radiation sickness if received within 24 hours (1000 mSv) [49]. Because this dissertation studied the maximum concentrations resulting from cyclotron operation, only ^{11}C and ^{18}F were used for modelling. Other cyclotron-produced radionuclides at Tays would be ^{15}O and ^{13}N but compared to ^{11}C and ^{18}F, their production would result in lesser amount of released activity.

The choice of the model, input parameter values, assumptions and evaluated values affect the reliability of the obtained results. The choice of model was justifiable because concentrations of short-lived radionuclides were needed to be modelled in relatively short distances, up to a few hundred meters from the source, and no major terrain complexity was identified in the surroundings of the planned cyclotron location. The release rate values were calculated by using the real values met at Turku PET Centre and by estimating the cyclotron usage at Tays. All the input parameters for calculating the effective height were estimations, made after consulting Medical Physicist Korkola. The constants for determining the dispersion parameters were chosen based on the empirical findings of M. Smith [38]. Changing the choice of constants to another possible set [37] would have produced only a minor difference in results, especially when all the other estimations and averages used in calculations are considered. Only one value for wind speed was used for calculations, but the effect of different wind speeds on fall-out and concentration was studied. The obtained results are good estimates, but if the study was repeated, a recommended way to provide exact results would be to measure the released activities by exhaust detectors when actual data would be available instead of estimations. Obtained concentration

profiles gave a directional view of the concentration distribution in different planes but as the terrestrial elevation was not considered in the model, they cannot be directly used for individual point dose calculations. Gaussian plume model does not consider differences in terrain roughness, but they can easily be incorporated into the calculations when concentration is needed to find at a single point. If the produced calculation tool was utilized further for (regulatory) calculations, it would be recommended to consider the differences in elevation in relation to the sea level at individual points in the hospital environment, and hence to find the critical points for dose calculations. In practice, this would mean adding the difference between ground level height at the point of release and at the point of observation to the height of possible building or other interesting spot in terrain at the point of observation.

Regulative dose calculations require finding the radiation dose at individual critical points, e.g., nearby buildings. Such calculations were not however performed, i.e., the critical spots were not determined from the map, because for instance the exact planned location of the cyclotron and the chimney was not decided at the time of this project. Also, several estimates of the variable values, for example considering the gas release conditions, were used in the modelling. The regulative dose calculations required by STUK must be performed by a radiation safety officer afterwards the real situation is recognized. Also, the terrestrial elevation, neglected in this dissertation, must be considered in the determined critical calculation points.

6 Conclusions

This dissertation is concluded by considering the initial research questions and finally making an estimation of the success of this project:

1. *How to model the dose of a representative person when radioactive materials are needed to be released into the atmosphere from a medical cyclotron in general case?*
The most suitable atmospheric dispersion model for the studied situation was chosen by considering the properties of source, emission and environment, the meteorological conditions in the area, and the distance to be modelled. The model was then applied for calculating the concentrations downwind from the release, and to find the maximum concentrations at different heights from the ground. Maximum concentrations were finally used for calculating the total radiation dose of a representative person.

2. *Based on the simulations, is it safe to build a medical cyclotron in Tays campus area?*
Dose calculations revealed that in each three release scenarios, accidental leak of ^{11}C and normal release of ^{11}C and ^{18}F, the maximum allowed radiation dose limit was exceeded at some calculation points. In each case, the dose limit was exceeded only at height z = 32.4 m which corresponds the effective release height. In accidental leak of ^{11}C, the dose limit was exceeded up to 45 m away downwind from the source. In normal release, the limit was exceeded until 20 m and 40 m from the source with ^{11}C and ^{18}F, respectively. Therefore, no buildings, etc. with height $\geq$ the chimney height, with terrestrial elevation considered, should be placed within a 45 m radius from it. At present, there are no buildings of that height within a 45 m radius from the approximate planned site of the chimney. Additionally, it was noted that compared to other possible radiation doses received by the population, resulting, for example, from medical examinations or from background radiation, the maximum doses calculated here were significantly smaller. Therefore, with the values used for dose calculations in this dissertation, building a cyclotron in Tays campus area would not be unsafe as no one stays in the area where the radiation dose limit would be exceeded.

This dissertation did not take a position on whether it would really be safe to place

a cyclotron in the Tays area. The knowledge about location of the exhaust chimney was limited, and therefore it was not reasonable to determine the critical buildings or areas in its environment and further use those points for calculating the dose of a representative person. Also, determining the critical calculation points would have required considering terrestrial elevation in the calculations. The regulatory dose calculations required by STUK must be performed by a radiation safety officer when the Tays cyclotron project will proceed. Hence, this was a hypothetical study which may not represent the possible future situation at Tays. This dissertation was however successful, because a calculation tool which, with slight modifications, can be used for more precise dose calculations in Tays case but also generally. The calculations also gave a good estimate of the magnitude of the doses resulting from such cyclotron operation.

References

[1] M. Giardina, E. Tomarchio and D. Greco, "Analysis of radionuclide concentration in air released through the stack of a radiopharmaceutical production facility based on a medical cyclotron," *Radiat. Phys. Chem.*, vol. 116, pp. 368–372, 2015.

[2] A. Sowa, I. Jackson, T. Desmond, J. Alicea, A. Mufarreh, J. Pham, J. Stauff, W. Winton, M. Fawaz, B. Henderson, B. Hockley, V. Rogers, R. Koeppe and P. Scott, "Futureproofing [^{18}F]fludeoxyglucose manufacture at an Academic Medical Center," *EJNMMI Radiopharm. Chem.*, vol. 3, pp. 1–12, 2018.

[3] B. Mukherjee, "A real-time positron monitor for the estimation of stack effluent releases from PET medical cyclotron facilities," *Appl. Radiat. Isot.*, vol. 57, pp. 899–905, 2002.

[4] A. Khlaifi, S. Dahech, G. Beltrando, A. Ionescua and Y. Candaua, "Spatial dispersion modelling of SO_2 according to the atmospheric circulation in a coastal city: Sfax (Tunisia)," *Meteorol. Appl.*, vol. 15, pp. 513–522, 2008.

[5] P. He, B. Zheng and J. Zheng, "Urban PM2.5 diffusion analysis based on the improved gaussian smoke plume model and support vector machine," *Aerosol Air Qual. Res.*, vol. 18, pp. 3177–3186, 2018.

[6] T. Peltonen and J. Lahtinen. "Tiuku: Collaborative emergency management tool." (Presented at Cores symposium, Tampere University, 6.9.2018).

[7] S. Vallabhajosula, "Radiopharmaceuticals for PET," in *Clinical Nuclear Medicine*, H. J. Biersack and L. M. Freeman, Eds., Berlin: Springer, 2007, p. 59.

[8] S. R. Cherry, J. A. Sorenson and M. E. Phelps, *Physics in Nuclear Medicine*, 4th ed. London: Elsevier, 2014, pp. 48–57.

[9] P. J. Scott, "Methods for the incorporation of carbon-11 to generate radiopharmaceuticals for PET imaging," *Angew. Chem. Int. Ed.*, vol. 48, pp. 6001–6004, 2009.

[10] J. S. Wilson, M. A. Avila-Rodriguez, R. R. Johnson, A. Zyuzin and S. A. McQuarrie, "Niobium sputtered havar foils for the high-power production of reactive [^{18}F]fluoride by proton irradiation of [^{18}O]H_2O targets," *Appl. Radiat. Isot.*, vol. 66, pp. 565–570, 2008.

[11] L. Cai, S. Lu and W. Pike, "Chemistry with [^{18}F]fluoride ion," *Eur. J. Org. Chem.*, vol. 2008, pp. 2853–2873, 2008.

[12] H. Zhuang and I. Codreanu, "Growing applications of FDG PET-CT imaging in non-oncologic conditions," *J. Biomed. Res.*, vol. 29, pp. 189–202, 2015.

[13] H. A. Nabi and J. M. Zubeldia, "Clinical applications of ^{18}F-FDG in oncology," *J. Nucl. Med. Technol.*, vol. 30, pp. 3–9, 2002.

[14] E. Santos and S. Khan, "A novel approach to gaseous waste treatment in a nuclear medicine facility," *Int. J. Sci. Environ. Technol.*, vol. 16, pp. 1–6, 2019.

[15] G. Antoni, "Development of carbon-11 labelled PET tracers - radiochemical and technological challenges in a historic perspective," *J. Label. Compd. Radiopharm.*, vol. 58, pp. 65–72, 2015.

[16] J. C. Clark, C. Crouzel, G. J. Meyer and K. Strijckmans, "Current methodology for oxygen-15 production for clinical use," *Int. J. Rad. Appl. Instr. A.*, vol. 38, pp. 597–600, 1987.

[17] F. A. Mettler and M. J. Guiberteau, "Cardiovascular system," in *Essentials of Nuclear Medicine and Molecular Imaging*, Amsterdam: Elsevier, 2018, pp. 116–174.

[18] T. Koskela, "Soveltuuko käyttäytymisterapia terveyspalveluiden suurkäyttäjille?" *Duodecim*, vol. 132, p. 1945, 2016.

[19] P. Korkola. "Tays uudistamisohjelma, syklotronihanke, esiselvitys." (2018, [Updated 6 Sept 2018, Cited 31 Oct 2022]), [Online]. Available: https://www.tays.fi/fi-FI.

[20] S. Surti, V. Viswanath, M. E. Daube-Witherspoon, M. Conti, M. E. Casey and J. S. Karp, "Benefit of improved performance with state-of-the art digital PET/CT for lesion detection in oncology," *J. Nucl. Med.*, vol. 61, pp. 1684–1690, 2020.

[21] M. S. Hofman, N. Lawrentschuk, R. J. Francis, C. Tang, I. Vela, P. Thomas, N. Rutherford, J. M. Martin, M. Frydenberg, R. Shakher, L. M. Wong, K. Taubman, S. Ting Lee, E. Hsiao, P. Roach, M. Nottage, I. Kirkwood, D. Hayne, E. Link, P. Marusic, A. Matera, A. Herschtal, A. Iravani, R. J. Hicks, S. Williams and D. G. Murphy, "Prostate-specific membrane antigen PET-CT in patients with high-risk prostate cancer before curative-intent surgery

or radiotherapy (proPSMA): A prospective, randomised, multicentre study," *Lancet*, vol. 395, pp. 1208–1216, 2020.

[22] L. Kestilä and S. Karvonen, *Suomalaisten Hyvinvointi 2018*. Helsinki: Terveyden ja Hyvinvoinnin Laitos THL, 2019, pp. 46–58.

[23] J. Knuuti, "PET-kuvantaminen tänään ja tulevaisuudessa," *Duodecim*, vol. 136, pp. 1059–61, 2020.

[24] C. Pascali, V. De Sanctis, C. Chiesa, A. Bogni, F. Crippa, R. Marchesini and E. Bombardieri, "A system for the automatic monitoring and safe disposal of short-lived radioactive gaseous compounds from hot-cells in a PET facility," *Appl. Radiat. Isot.*, vol. 47, pp. 717–722, 1996.

[25] Radiation and Nuclear Safety Authority (STUK). "Radioactive waste and discharges from unsealed sources, ST Guide 6.2." (2017, [Updated 9 Jan 2017; Cited 31 Oct 2022]), [Online]. Available: https://www.stuklex.fi/en/ohje/ST6-2.

[26] H. D. Brenk, J. E. Fairobent and E. H. Markee, "Transport of radionuclides in the atmosphere," in *Radiological assessment. A Textbook on Environmental Dose Assessment*, J. E. Till and H. R. Meyer, Eds., Rockville: U.S. Nuclear Regulatory Commission, 1983, p. 60.

[27] A. De Visscher, *Air Dispersion Modelling: Foundations and Applications*, 1st ed. Hoboken: Wiley, 2013, pp. 1–4, 141–200.

[28] G. E. Start and L. L. Wendell, "Regional effluent dispersion calculations considering spatial and temporal meteorological variations," *NOAA Tech. Memo.*, vol. 44, pp. 1–41, 1974.

[29] A. Leelossy, F. Molnár, F. Izsák, Á. Havasi, I. Lagzi and R. Mészáros, "Dispersion modeling of air pollutants in the atmosphere: A review," *Open Geosci.*, vol. 6, pp. 257–278, 2014.

[30] F. A. Gifford, "An outline of theories of diffusion in the lower layers of the atmosphere," in *Meteorology and Atomic Energy, 1968*, D. H. Slade, Ed., Oak Ridge: Environmental Science Services Administration, 1968, pp. 66–116.

[31] S. R. Hanna, G. A. Briggs and R. P. Hosker, *Handbook on Atmospheric Diffusion*. Washington, D.C.: U.S. Department of Energy, 1982.

[32] G. A. Briggs, *Diffusion Estimation for Small Emissions. Preliminary Report*. Oak Ridge: National Oceanic, Atmospheric Administration, Air Resources Atmospheric Turbulence and Diffusion Laboratory, 1973.

[33] F. Pasquill, "The estimation of the dispersion of windborne material," *Meteorol. Mag.*, vol. 90, pp. 33–49, 1961.

[34] F. A. Gifford, "Use of routine meteorological observations for estimating atmospheric dispersion," *Nucl. Saf.*, vol. 2, pp. 47–57, 1961.

[35] D. B. Turner, "A diffusion model for an urban area," *J. Appl. Meteorol.*, vol. 3, pp. 83–91, 1964.

[36] D. B. Turner, *Workbook of Atmospheric Dispersion Estimates*, 2nd ed. Boca Raton: CRC Press, 1994.

[37] J. L. McElroy, "A comparative study of urban and rural dispersion," *J. Appl. Meteorol.*, vol. 8, pp. 19–31, 1969.

[38] M. E. Smith, *Recommended Guide for the Prediction of the Dispersion of Airborne Effluents*, 1st ed. New York: American Society of Mechanical Engineers, 1968.

[39] G. S. Raynor, R. M. Brown and S. Sethuraman, "A comparison of diffusion from a small island and an undisturbed ocean site," *J. Appl. Meteorol.*, vol. 17, pp. 129–139, 1978.

[40] G. A. Briggs, "Plume rise predictions," in *Lectures on Air Pollution and Environmental Impact Analyses*, D. A. Haugen, Ed., Boston: American Meteorological Society, 1982, pp. 59–111.

[41] G. A. Briggs, "Plume rise and buoyancy effects," in *Atmospheric Science and Power Production*, D. Randerson, Ed., Washington, D.C.: U.S. Department of Energy, 1984, pp. 327–366.

[42] G. A. Briggs, *Plume rise*. Oak Ridge: U.S. Atomic Energy Commission, Division of Technical Information, 1969.

[43] G. A. Briggs, *Some Recent Analyses of Plume Rise Observation*. Oak Ridge: National Oceanic, Atmospheric Administration, Air Resources Atmospheric Turbulence and Diffusion Laboratory, 1970.

[44] G. A. Briggs, "Chimney plumes in neutral and stable surroundings," *Atmos. Environ.*, vol. 6, pp. 507–510, 1972.

[45] G. J. Balady, R. Arena, K. Sietsema, J. Myers, L. Coke, G. F. Fletcher, D. Forman, B. Franklin, M. Guazzi, M. Gulati, S. J. Keteyian, C. J. Lavie, R. Macko, D. Mancini and R. V. Milani, "Clinician's guide to cardiopulmonary exercise testing in adults: A scientific statement from the american heart association," *Circulation*, vol. 122, pp. 191–225, 2010.

[46] H. Tikkanen and J. Peltonen, "Liikunta ja keuhkot," *Duodecim*, vol. 117, pp. 639–646, 2001.

[47] K. Eckerman, J. Harrison, H. G. Menzel and C. H. Clement, "Icrp publication 119: Compendium of dose coefficients based on icrp publication 60," *Ann. ICRP*, vol. 42, p. 25, 2012.

[48] D. C. Kocher, "Dose-rate conversion factors for external exposure to photons and electrons," *Health Phys.*, vol. 45, pp. 665–686, 1983.

[49] Radiation and Nuclear Safety Authority (STUK). "Examples of radiation doses and external dose rates." (2021, [Updated 26 Jul 2021; Cited 31 Oct 2022]), [Online]. Available: https://www.stuk.fi/web/en/topics/emergencies/examples-of-radiation-doses-and-external-dose-rates.

A Materials

A.1 Wind Roses

Figure 9 shows the wind roses which describe the wind statistics at two measurement stations at Tampere: Siilinkari (a) and Tampere-Pirkkala Airport (b). The wind roses were provided by the Finnish Meteorological Institute (E. Tuovinen, personal communication, February 7, 2022). The measured 10-year average wind speeds at Siilinkari and Tampere-Pirkkala Airport were 5.0 and 3.0 m/s, respectively.

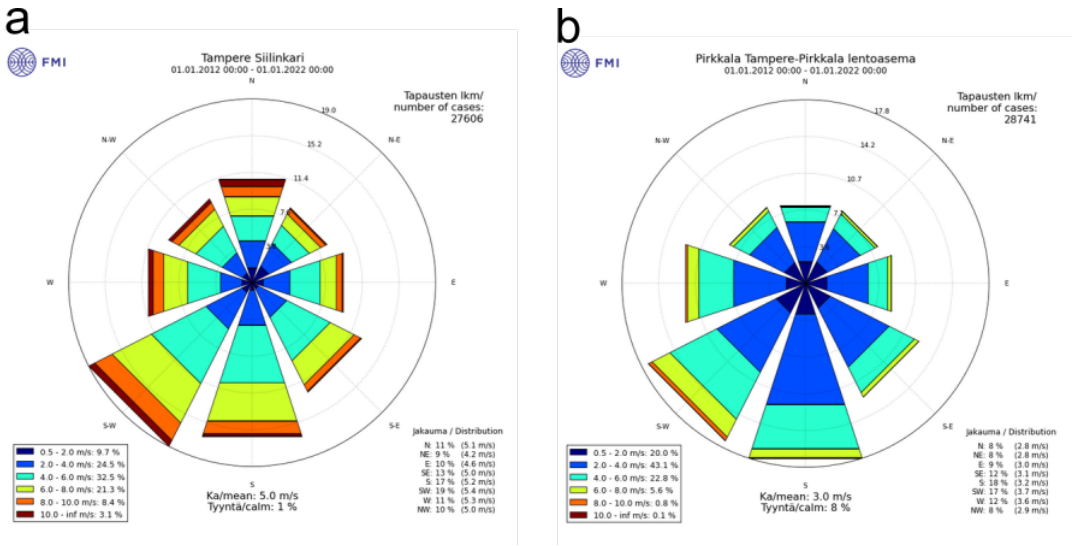

Figure 9. Wind roses describing the wind statistics at Tampere. At Siilinkari measurement station (a), the average wind speed is 5.0 m/s. At Tampere-Pirkkala Airport measurement station (b), the average wind speed is 3.0 m/s.

A.2 Release Rates

Step-by-step solution for calculating the release rates (Bq/s) from the released activities (Bq) is presented in Figure 10. In accidental leak, Q was obtained by dividing the released activity by the duration of the release. In normal release, Q was calculated from the annual released activity by considering the number of synthesis days and the duration of the synthesis.

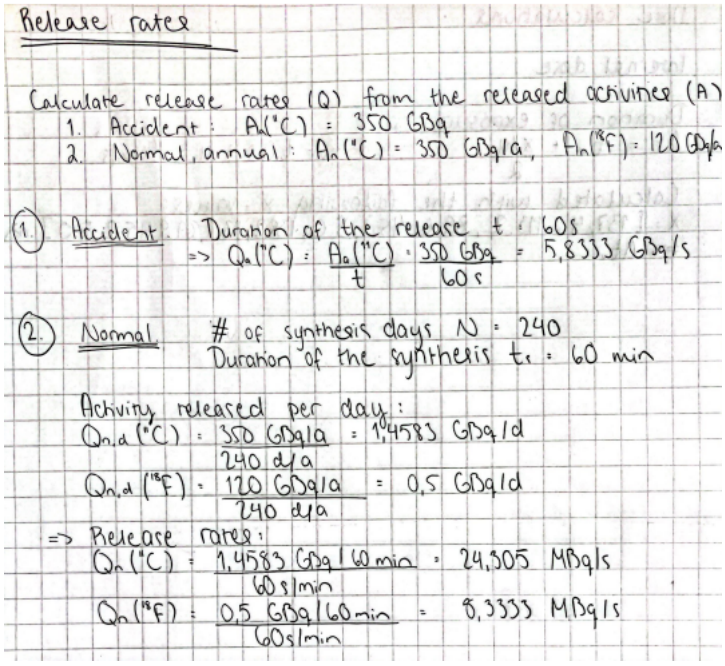

Figure 10. Step-by-step solution for calculating the release rate from the released activities in each release scenario. In accidental leak, the release rate was found by dividing the released activity by the duration of the release. In normal release, the annual release rate was found by considering the amount of synthesis days and the duration of the synthesis.

A.3 Example Code

```
% This is an example code which shows how to draw air pollutant
% concentration profiles. Calculations are based on Gaussian plume
% equation. Variable values used in this example are chosen based on a
% schematic situation where accidental leak of carbon-11 isotope would occur
% at Tampere University Hospital during a cyclotron operation.

% Enter the values for release rate Q [Bq/s], half-live of the studied isotope t_half (s);
% mean wind speed u (m/s), % receptor height z (m) and physical source height h (m).
Q=5.83333*10^9; t_half=1219.8; u=4; h=30; z=0;

% Enter the values for dispersion coefficients. The values depend on
% atmospheric stability, source type and surface roughness. Here chosen for
% 'high stacks, smooth to medium rough surface', Ref. Smith, M. 1968.
a=0.36; b=0.86; c=0.33; d=0.86;

% Choose the range and interval for direction of the wind x (m) and
% horizontal direction perpendicular to the wind y (m). y=0 at the center
% of the plume; positive on your left when you look downwind).
x=40:0.1:200;
y=-110:0.1:110;

% Create 2-D grid coordinates based on the coordinates contained in vectors x and y.
[x,y]=meshgrid(x,y);

% Enter gravitational acceleration g (m/s^2), plume exit velocity V_s
% (m/s), stack diameter D_s (m), temperature of the gas T_s (K) and
% temperature of the environment T (K):
g=9.81; V_s=4; D_s=0.8; T_s=293.15; T=277.55;
```

```
% Plume rise calculation

% Buoyancy flux parameter:
F=(g/4)*V_s*D_s.^(2)*((T_s-T)/T_s);

% Downwind distance at which plume rise reaches its maximum:
x_f=49*F^(5/8);
% At distances x > x_f plume rise is calculated as (otherwise replace x_f
% with x --> results in rise1, rise2):
rise2=(1.6*F^(1/3)*x_f.^(2/3))/4;

% Effective height:
h_eff=h+rise2;
```

```
% Horizontal (y) and vertical (z) dispersion parameters:
sigma_yb=a.*x.^b;
sigma_zb=c.*x.^d;

% Terms in Gaussian plume equation:
term1=Q./(2*pi*u*sigma_yb.*sigma_zb);
term2=exp((-1/2)*(y.^2)./(sigma_yb).^2);
term3=exp((-1/2).*((z-h_eff).^2)./(sigma_zb).^2);
```

1

```
% Radioactivity concentration (Bq/m^3):
c=term1.*term2.*term3;
% Correction for radioactive decay:
lambda=0.693./t_half;
t=x./u;
DF=exp(-lambda.*t);
c=DF.*c;

% Find the maximum concentration:
[row, col] = find(ismember(c, max(c(:))));
c(row,col);
```

```
% Draw a colormap describing the xy concentration profile
Z = c;
f=figure;
% Create a figure without displaying it:
set(f,'Visible', 'off');
hold on;
s1 = subplot(2, 1, 1);
contourf(x,y,Z,'edgecolor','none');
title('Concentration profile with {\it z} = 0 m','FontSize', 8);
xlabel('{\it x} [m]');
ylabel('{\it y} [m]');
colorbar;
h=colorbar;
ylabel(h, 'Concentration range (Bq/m^3)');

% Concentration profile with different color intervals:
s2 = subplot(2, 1, 2);
color = [[1.0, 1.0, 1.0],
         [0.0, 1.0, 0.0],
         [0.0, 0.0, 1.0],
         [0.0, 1.0, 1.0],
         [1.0, 0.0, 1.0],];
colormap(s2, color);
contourf(x,y,Z, [1000, 10^4, 10^5], 'edgecolor', 'none');
title('Concentration profile with {\it z} = 0 m','FontSize', 8);
xlabel('{\it x} [m]');
ylabel('{\it y} [m]');
hold off
```

B Results

B.1 Concentrations Around Plume Centreline

^{11}C concentrations (Bq/m^3) in accidental leak calculated with different *xy* combinations at five heights are presented in tables 3–7. The strikethrough results represent concentrations values under one thousandth of the maximum concentration at each height. At x = 0 m, no concentrations to be considered occurred at any height. At heights z = 0, 5, 10 and 20 m, concentrations greater than one thousandth of the maximum occurred up to 90 m from the plume centreline. At the level of the effective height of release, concentrations > 1 ‰ of the maximum at that height occurred up to y = 70 m.

Table 3. ^{11}C concentrations (Bq/m^3) with several *xy* combinations in accidental leak at the ground-level, z = 0 m. Concentrations over 1‰ of the ground level maximum concentration, 1.5×10^5 Bq/m^3, began to occur from x = 40 m. With increasing x, concentrations over 1‰ of the maximum were found further away from the plume centreline, up to y = 90 m.

x [m] \ y [m]	0	10	20	30	40	50	60	70	80	90	100
20	~~1.6×10^5~~										
30	~~5.5~~										
40	738.2	375.0	~~49.1~~								
50	7.4×10^3	4.7×10^3	1.2×10^3	~~116.2~~							
60	2.5×10^4	1.8×10^4	6.6×10^3	1.2×10^3	~~115.0~~						
70	5.2×10^4	4.0×10^4	1.8×10^4	5.0×10^3	823.6	~~80.3~~					
80	7.9×10^4	6.5×10^4	3.5×10^4	1.2×10^4	3.0×10^3	465.37	~~48.5~~				
90	1.0×10^5	8.8×10^4	5.3×10^4	2.3×10^4	7.1×10^3	1.6×10^3	245.7	~~27.7~~			
100	1.2×10^5	1.1×10^5	7.0×10^4	3.5×10^4	1.3×10^4	3.7×10^3	788.5	~~127.6~~			
110	1.3×10^5	1.2×10^5	8.4×10^4	4.6×10^4	2.0×10^4	6.9×10^3	1.9×10^3	397.6	~~66.8~~		
120	1.4×10^5	1.3×10^5	9.5×10^4	5.7×10^4	2.8×10^4	1.1×10^4	3.6×10^3	943.9	203.3	~~35.7~~	
130	1.5×10^5	1.3×10^5	1.0×10^5	6.5×10^4	3.5×10^4	1.6×10^4	5.9×10^3	1.8×10^3	484.0	~~106.2~~	
140	1.5×10^5	1.4×10^5	1.1×10^5	7.2×10^4	4.2×10^4	2.1×10^4	8.7×10^3	3.1×10^3	962.4	253.3	~~57.0~~
150	1.5×10^5	1.4×10^5	1.1×10^5	7.7×10^4	4.8×10^4	2.5×10^4	1.2×10^4	4.8×10^3	1.7×10^3	510.6	~~135.7~~

Table 4. ^{11}C concentrations (Bq/m^3) with several *xy* combinations in accidental leak at z = 5 m. Concentrations over 1‰ of the maximum concentration at this height, 2.1×10^5 Bq/m^3, began to occur from x = 30 m. With increasing x, concentrations over 1‰ of the maximum were found further away from the plume centreline, up to y = 90 m.

x [m] \ y [m]	0	10	20	30	40	50	60	70	80	90	100
20	~~0.0~~										
30	283.1	~~93.2~~									
40	8.2×10^3	4.2×10^3	545.3	~~18.4~~							
50	3.8×10^4	2.4×10^3	6.0×10^3	598.8	~~23.7~~						
60	8.4×10^4	6.0×10^4	2.2×10^4	4.0×10^3	381.2	~~18.3~~					
70	1.3×10^5	1.0×10^5	4.6×10^4	1.3×10^4	2.1×10^3	~~201.2~~					
80	1.6×10^5	1.3×10^5	7.2×10^4	2.6×10^4	6.1×10^3	966.2	~~100.6~~				
90	1.9×10^5	1.6×10^5	9.6×10^4	4.2×10^4	1.3×10^4	2.8×10^3	446.2	~~50.2~~			
100	2.0×10^5	1.7×10^5	1.1×10^5	5.7×10^4	2.1×10^4	6.1×10^3	1.3×10^3	209.9	~~25.7~~		
110	2.1×10^5	1.8×10^5	1.3×10^5	7.1×10^4	3.1×10^4	1.1×10^4	2.8×10^3	606.6	~~101.9~~		
120	2.0×10^5	1.8×10^5	1.4×10^5	8.2×10^4	4.0×10^4	1.6×10^4	5.1×10^3	1.4×10^3	292.4	~~51.3~~	
130	2.0×10^5	1.8×10^5	1.4×10^5	9.0×10^4	4.8×10^4	2.2×10^4	8.1×10^3	2.5×10^3	664.5	~~145.8~~	
140	1.9×10^5	1.8×10^5	1.4×10^5	9.6×10^4	5.5×10^4	2.7×10^4	1.1×10^4	4.1×10^3	1.3×10^3	334.8	~~75.3~~
150	1.9×10^5	1.7×10^5	1.4×10^5	9.9×10^4	6.1×10^4	3.2×10^4	1.5×10^4	6.1×10^3	2.1×10^3	654.2	~~173.9~~

Table 5. ^{11}C concentrations (Bq/m^3) with several *xy* combinations in accidental leak at z = 10 m. Concentrations over 1‰ of the maximum concentration at this height, 3.1×10^5 Bq/m^3, began to occur from x = 30 m. With increasing x, concentrations over 1‰ of the maximum were found further away from the plume centreline, up to y = 90 m.

x [m] \ y [m]	0	10	20	30	40	50	60	70	80	90	100
20	~~28.0~~										
30	7.6×10^3	2.5×10^3	~~88.9~~								
40	6.1×10^4	3.1×10^4	4.0×10^3	~~136.7~~							
50	1.5×10^5	9.4×10^4	2.4×10^4	2.3×10^3	~~92.7~~						
60	2.3×10^5	1.6×10^5	5.9×10^4	1.1×10^4	1.0×10^3	~~49.7~~					
70	2.8×10^5	2.2×10^5	9.9×10^4	2.7×10^4	4.4×10^3	432.6	~~25.1~~				
80	3.0×10^5	2.5×10^5	1.3×10^5	4.8×10^4	1.1×10^4	1.8×10^3	~~184.9~~				
90	3.1×10^5	2.6×10^5	1.6×10^5	6.8×10^4	2.1×10^4	4.6×10^3	733.2	~~82.7~~			
100	3.0×10^5	2.6×10^5	1.7×10^5	8.6×10^4	3.2×10^4	9.2×10^3	2.0×10^3	317.7	~~38.9~~		
110	2.9×10^5	2.6×10^5	1.8×10^5	1.0×10^5	4.4×10^4	1.5×10^4	4.0×10^3	862.3	~~144.9~~		
120	2.8×10^5	2.5×10^5	1.8×10^5	1.1×10^5	5.4×10^4	2.1×10^4	7.0×10^3	1.8×10^3	395.8	~~69.5~~	
130	2.6×10^5	2.4×10^5	1.8×10^5	1.2×10^5	6.3×10^4	2.8×10^4	1.1×10^4	3.3×10^3	865.1	~~189.9~~	
140	2.4×10^5	2.3×10^5	1.8×10^5	1.2×10^5	7.0×10^4	3.4×10^4	1.4×10^4	5.2×10^3	1.6×10^3	422.3	~~95.0~~
150	2.3×10^5	2.1×10^5	1.7×10^5	1.2×10^5	7.5×10^4	4.0×10^4	1.9×10^4	7.5×10^3	2.6×10^3	804.0	~~213.7~~

Table 6. ^{11}C concentrations (Bq/m^3) with several *xy* combinations in accidental leak at z = 20 m. Concentrations over 1‰ of the maximum concentration at this height, 1.0×10^6 Bq/m^3, began to occur from x = 20 m. With increasing x, concentrations over 1‰ of the maximum were found further away from the plume centreline, up to y = 90 m.

x [m] \ y [m]	0	10	20	30	40	50	60	70	80	90	100
0	~~†~~										
10	~~535.4~~										
20	2.4×10^5	2.6×10^4	~~31.8~~								
30	7.4×10^5	2.5×10^5	8.7×10^3 ~~33.8~~								
40	10.0×10^5	5.1×10^5	6.6×10^4	2.2×10^3	~~19.6~~						
50	1.0×10^6	6.3×10^5	1.6×10^5	1.6×10^4	~~623.7~~						
60	9.2×10^5	6.6×10^5	2.4×10^5	4.4×10^4	4.2×10^3	~~200.0~~					
70	8.1×10^5	6.3×10^5	2.9×10^5	7.9×10^4	1.3×10^3	1.3×10^3	~~73.2~~				
80	7.1×10^5	5.8×10^5	3.1×10^5	1.1×10^5	2.6×10^4	4.1×10^3	~~432.3~~				
90	6.2×10^5	5.2×10^5	3.2×10^5	1.4×10^5	4.2×10^4	9.3×10^3	1.5×10^3	~~165.4~~			
100	5.4×10^5	4.7×10^5	3.1×10^5	1.5×10^5	5.8×10^4	1.6×10^4	3.5×10^3	~~566.6~~			
110	4.8×10^5	4.3×10^5	3.0×10^5	1.6×10^5	7.1×10^4	2.4×10^4	6.6×10^3	1.4×10^3	~~236.8~~		
120	4.2×10^5	3.8×10^5	2.8×10^5	1.7×10^5	8.2×10^4	3.3×10^4	1.1×10^4	2.8×10^3	~~604.2~~		
130	3.8×10^5	3.4×10^5	2.6×10^5	1.7×10^5	9.0×10^4	4.1×10^4	1.5×10^4	4.8×10^3	1.3×10^3	~~274.5~~	
140	3.4×10^5	3.1×10^5	2.5×10^5	1.7×10^5	9.6×10^4	4.7×10^4	2.0×10^4	7.2×10^3	2.2×10^3	~~584.1~~	
150	3.0×10^5	2.8×10^5	2.3×10^5	1.6×10^5	10.0×10^4	5.3×10^4	2.5×10^4	10.0×10^3	3.5×10^3	1.1×10^3	~~285.0~~

Table 7. ^{11}C concentrations (Bq/m^3) with several *xy* combinations in accidental leak at h_{eff}, z = 32.4 m. Concentrations over 1‰ of the maximum concentration at this height, 6.1×10^7 Bq/m^3, began to occur from x = 0–10 m. With increasing x, concentrations over 1‰ of the maximum were found further away from the plume centreline, up to y = 70 m.

x [m] \ y [m]	0	10	20	30	40	50	60	70	80
0	~~†~~								
10	3.4×10^7	2.2×10^4	~~5.7×10^6~~						
20	1.1×10^7	1.2×10^6	~~1.5×10^5~~						
30	5.6×10^6	1.8×10^6	6.6×10^4	~~254.6~~					
40	3.4×10^6	1.7×10^6	2.3×10^5	~~7.7×10^5~~					
50	2.3×10^6	1.5×10^6	3.7×10^5	3.6×10^4	~~1.4×10^5~~				
60	1.7×10^6	1.2×10^6	4.4×10^5	8.1×10^4	~~7.7×10^5~~				
70	1.3×10^6	1.0×10^6	4.6×10^5	1.3×10^5	2.1×10^4	~~2.0×10^5~~			
80	1.0×10^6	8.4×10^5	4.5×10^5	1.6×10^5	3.8×10^4	~~6.0×10^5~~			
90	8.4×10^5	7.1×10^5	4.3×10^5	1.9×10^5	5.7×10^4	1.3×10^4	~~2.0×10^5~~		
100	7.0×10^5	6.1×10^5	4.0×10^5	2.0×10^5	7.4×10^4	2.1×10^4	~~4.3×10^5~~		
110	5.9×10^5	5.3×10^5	3.7×10^5	2.0×10^5	8.8×10^4	3.0×10^4	~~8.2×10^5~~		
120	5.1×10^5	4.6×10^5	3.4×10^5	2.0×10^5	9.9×10^4	3.9×10^4	1.3×10^4	~~3.4×10^5~~	
130	4.4×10^5	4.1×10^5	3.1×10^5	2.0×10^5	1.1×10^5	4.8×10^4	1.8×10^4	~~5.6×10^5~~	
140	3.9×10^5	3.6×10^5	2.8×10^5	1.9×10^5	1.1×10^5	5.5×10^4	2.3×10^4	~~8.3×10^5~~	
150	3.5×10^5	3.2×10^5	2.6×10^5	1.8×10^5	1.1×10^5	6.0×10^4	2.8×10^4	1.1×10^4	~~4.0×10^5~~

B.2 Intermediate Results

The intermediate results used for the dose calculations are presented in this section. The values corresponding to each release scenarios, accidental leak of ^{11}C, normal release of ^{11}C and normal release of ^{18}F, are presented in Tables 8–10, respectively. The values for duration of emission, inhaled air volume and inhaled activity are presented here for each point of observation. The point of observation in the first column on the right corresponds to a calculation point used in the dose calculations. The second column describes duration of the exposure Δt, calculated by Equation (15). In the third column, values for V_{i}, calculated by Equation (14) are shown. The inhaled activities, calculated by Equation (13) at each calculation point are presented in the fourth column.

Table 8. Intermediate results for the dose calculations in accidental leak of ^{11}C: The values for Δt, V_i and a were calculated using Equations (13)–(15) and they are presented at each calculation point (x, y, z).

Point of observation (x, y, z)	Δt (s)	V_i (m^3)	a (Bq)
137.4,0,0	77.175	0.0193	2.8303×10^{3}
137.4,10,0	77.175	0.0193	2.6095×10^{3}
137.4,20,0	77.175	0.0193	2.0453×10^{3}
137.4,30,0	77.175	0.0193	1.3628×10^{3}
137.4,40,0	77.175	0.0193	771.9235
137.4,50,0	77.175	0.0193	371.6896
137.4,60,0	77.175	0.0193	152.1439
137.4,70,0	77.175	0.0193	52.9416
137.4,80,0	77.175	0.0193	15.6606
137.4,90,0	74.15	0.0193	3.9381
113.2,0,5	74.15	0.01854	3.8168×10^{3}
113.2,10,5	74.15	0.01854	3.4078×10^{3}
113.2,20,5	74.15	0.01854	2.4254×10^{3}
113.2,30,5	74.15	0.01854	1.3762×10^{3}
113.2,40,5	74.15	0.01854	622.4239
113.2,50,5	74.15	0.01854	224.4157
113.2,60,5	74.15	0.01854	64.5013
113.2,70,5	74.15	0.01854	14.7785
113.2,80,5	74.15	0.01854	2.6993
89.6,0,10	71.2	0.0178	5.5056×10^{3}
89.6,10,10	71.2	0.0178	4.6471×10^{3}
89.6,20,10	71.2	0.0178	2.7945×10^{3}
89.6,30,10	71.2	0.0178	1.1973×10^{3}
89.6,40,10	71.2	0.0178	365.4561
89.6,50,10	71.2	0.0178	79.4745
89.6,60,10	71.2	0.0178	12.3133
45.1,0,20	65.6375	0.0164	1.6714×10^{4}
45.1,10,20	65.6375	0.0164	9.6129×10^{3}
45.1,20,20	65.6375	0.0164	1.8288×10^{3}
45.1,30,20	65.6375	0.0164	115.0882
45.1,40,20	65.6375	0.0164	2.3957
45.1,50,20	65.6375	0.0164	0.0165
5,0, 32.3538	60.625	0.0152	9.3902×10^{5}
5,10, 32.3538	60.625	0.0152	1.2108×10^{-5}
10,0,32.3538	61.25	0.0153	5.2208×10^{5}
15,0,32.3538	61.875	0.0155	2.8427×10^{5}
20,0,32.3538	62.5	0.0156	2.0842×10^{5}
25,0,32.3538	63.125	0.0158	1.2204×10^{5}
30,0,32.3538	63.75	0.0159	8.9589×10^{5}
35,0,32.3538	64.375	0.0161	6.9481×10^{4}
40,0,32.3538	65	0.0163	5.5836×10^{4}
45,0,32.3538	65.625	0.0164	4.5822×10^{4}

Table 9. Intermediate results for the dose calculations in normal release of ^{11}C: The values for Δt, V_i and a were calculated using Equations (13)–(15) and they are presented at each calculation point (x, y, z).

Point of observation (x, y, z)	Δt (s)	V_i (m^3)	a (Bq)
137.4,0,0	3.6172×10^3	0.9043	552.5523
137.4,10,0	3.6172×10^3	0.9043	509.4515
137.4,20,0	3.6172×10^3	0.9043	399.3146
137.4,30,0	3.6172×10^3	0.9043	266.0559
137.4,40,0	3.6172×10^3	0.9043	150.6991
137.4,50,0	3.6172×10^3	0.9043	72.5659
137.4,60,0	3.6172×10^3	0.9043	29.7025
137.4,70,0	3.6172×10^3	0.9043	10.3356
137.4,80,0	3.6172×10^3	0.9043	3.0573
137.4,90,0	3.6172×10^3	0.9043	0.7688
113.2,0,5	3.6142×10^3	0.9036	775.0829
113.2,10,5	3.6142×10^3	0.9036	692.0225
113.2,20,5	3.6142×10^3	0.9036	492.5197
113.2,30,5	3.6142×10^3	0.9036	279.4664
113.2,40,5	3.6142×10^3	0.9036	126.3957
113.2,50,5	3.6142×10^3	0.9036	45.5712
113.2,60,5	3.6142×10^3	0.9036	13.0981
113.2,70,5	3.6142×10^3	0.9036	3.0011
113.2,80,5	3.6142×10^3	0.9036	0.5481
89.6,0,10	3.6112×10^3	0.9028	1.1634×10^3
89.6,10,10	3.6112×10^3	0.9028	982.0658
89.6,20,10	3.6112×10^3	0.9028	590.5839
89.6,30,10	3.6112×10^3	0.9028	253.0196
89.6,40,10	3.6112×10^3	0.9028	77.2290
89.6,50,10	3.6112×10^3	0.9028	16.7952
89.6,60,10	3.6112×10^3	0.9028	2.6021
45.1,0,20	3.6056×10^3	0.9014	3.8279×10^3
45.1,10,20	3.6056×10^3	0.9014	2.2014×10^3
45.1,20,20	3.6056×10^3	0.9014	418.8034
45.1,30,20	3.6056×10^3	0.9014	26.3559
45.1,40,20	3.6056×10^3	0.9014	0.5486
45.1,50,20	3.6056×10^3	0.9014	0.0038
5,0, 32.3538	3.6006×10^3	0.9002	2.3192×10^5
5,10,32.3538	3.6006×10^3	0.9002	2.9879×10^{-6}
10,0,32.3538	3.6012×10^3	0.9003	1.2803×10^5
15,0,32.3538	3.6019×10^3	0.9005	6.8809×10^4
20,0,32.3538	3.6025×10^3	0.9006	4.2536×10^4

Table 10. Intermediate results for the dose calculations in normal release of ^{18}F. The values for Δt, V_i and a were calculated using Equations (13)–(15) and they are presented at each calculation point (x, y, z)

Point of observation (x, y, z)	Δt (s)	V_i (m^3)	a (Bq)
138.2,0,0	3.6173×10^3	0.9043	192.4891
138.2,10,0	3.6173×10^3	0.9043	177.6373
138.2,20,0	3.6173×10^3	0.9043	139.6106
138.2,30,0	3.6173×10^3	0.9043	93.4457
138.2,40,0	3.6173×10^3	0.9043	53.2667
138.2,50,0	3.6173×10^3	0.9043	25.8588
138.2,60,0	3.6173×10^3	0.9043	10.6910
138.2,70,0	3.6173×10^3	0.9043	3.7643
138.2,80,0	3.6173×10^3	0.9043	1.1287
138.2,90,0	3.6173×10^3	0.9043	0.2883
113.7,0,5	3.6142×10^3	0.9035	269.2260
113.7,10,5	3.6142×10^3	0.9035	240.6230
113.7,20,5	3.6142×10^3	0.9035	171.7898
113.7,30,5	3.6142×10^3	0.9035	97.9710
113.7,40,5	3.6142×10^3	0.9035	44.6311
113.7,50,5	3.6142×10^3	0.9035	16.2412
113.7,60,5	3.6142×10^3	0.9035	4.7211
113.7,70,5	3.6142×10^3	0.9035	1.0962
89.9,0,10	3.6112×10^3	0.9028	403.0743
89.9,10,10	3.6112×10^3	0.9028	340.6627
89.9,20,10	3.6112×10^3	0.9028	205.6568
89.9,30,10	3.6112×10^3	0.9028	88.6830
89.9,40,10	3.6112×10^3	0.9028	27.3160
89.9,50,10	3.6112×10^3	0.9028	6.0099
89.9,60,10	3.6112×10^3	0.9028	0.9445
45.2,0,20	3.6057×10^3	0.9014	1.3192×10^3
45.2,10,20	3.6057×10^3	0.9014	761.9368
45.2,20,20	3.6057×10^3	0.9014	146.7949
45.2,30,20	3.6057×10^3	0.9014	9.4341
5,0,32.3538	3.6006×10^3	0.9002	7.9453×10^4
10,0,32.3538	61.25	0.0153	522219.6
15,0,32.3538	61.875	0.0155	284270
20,0,32.3538	62.5	0.0156	208416
25,0,32.3538	63.125	0.0158	122043.94
30,0,32.3538	63.75	0.0159	89588.55
35,0,32.3538	64.375	0.0161	69481.16
40,0,32.3538	65	0.0163	55835.65
45,0,32.3538	65.625	0.0164	45821.6
50,0,32.3538	66.25	0.0166	38644

B.3 Concentrations and Doses

All the calculated concentrations and the corresponding doses in accidental leak of ^{11}C and normal release of ^{11}C and ^{18}F are presented in Tables 11–13, respectively. The internal and external dose, D and E, were calculated from the concentration corresponding each point using Equations (12)–(16). The total dose at each point was calculated as a sum of internal and external dose.

Table 11. ^{11}C concentrations (Bq/m^3) and doses (μSv) in accidental leak. The total dose at each point of observation was found by adding up the internal and external doses.

Point of observation (x,y,z)	C (Bq/m^3)	D (μSv)	E (μSv)	D+E (μSv)
137.4,0.0,0.0	1.5×10^{5}	0.068	0.50	0.57
137.4,10.0,0.0	1.4×10^{5}	0.063	0.46	0.52
137.4,20.0,0.0	1.1×10^{5}	0.049	0.36	0.41
137.4,30.0,0.0	7.1×10^{4}	0.033	0.24	0.27
137.4,40.0,0.0	4.0×10^{4}	0.019	0.14	0.15
137.4,50.0,0.0	1.9×10^{4}	0.0089	0.065	0.074
137.4,60.0,0.0	7.9×10^{3}	0.0037	0.027	0.030
137.4,70.0,0.0	2.7×10^{3}	0.0013	0.0093	0.011
137.4,80.0,0.0	810	0.00038	0.0028	0.0031
137.4,90.0,0.0	200	0.000095	0.00069	0.00079
113.2,0.0,5.0	2.1×10^{5}	0.092	0.67	0.76
113.2,10.0,5.0	1.8×10^{5}	0.082	0.60	0.68
113.2,20.0,5.0	1.3×10^{5}	0.058	0.42	0.48
113.2,30.0,5.0	7.4×10^{4}	0.033	0.24	0.28
113.2,40.0,5.0	3.4×10^{4}	0.015	0.11	0.12
113.2,50.0,5.0	1.2×10^{4}	0.0054	0.039	0.045
113.2,60.0,5.0	3.5×10^{3}	0.0015	0.011	0.013
113.2,70.0,5.0	800	0.00035	0.0026	0.0030
113.2,80.0,5.0	150	0.000065	0.00047	0.00054
89.6,0.0,10.0	3.1×10^{5}	0.13	0.97	1.1
89.6,10.0,10.0	2.6×10^{5}	0.11	0.81	0.93
89.6,20.0,10.0	1.6×10^{5}	0.067	0.49	0.56
89.6,30.0,10.0	6.7×10^{4}	0.029	0.21	0.24
89.6,40.0,10.0	2.1×10^{4}	0.0088	0.064	0.073
89.6,50.0,10.0	4.5×10^{3}	0.0019	0.014	0.016
89.6,60.0,10.0	690	0.00030	0.0022	0.0025
45.1,0.0,20.0	1.0×10^{6}	0.40	2.9	3.3
45.1,10.0,20.0	5.9×10^{5}	0.23	1.7	1.9
45.1,20.0,20.0	1.1×10^{5}	0.044	0.32	0.37
45.1,30.0,20.0	7.0×10^{3}	0.0028	0.020	0.023
45.1,40.0,20.0	150	0.000058	0.00042	0.00048
45.1,50.0,20.0	1.0	4.0×10^{-7}	2.9×10^{-6}	3.3×10^{-6}
5.0,0.0, 32.4	6.2×10^{7}	23	170	190
5.0,10.0, 32.4	8.0×10^{-4}	2.9×10^{-10}	2.1×10^{-9}	2.4×10^{-9}
10.0,0.0,32.4	3.4×10^{7}	13	92	100
15.0,0.0,32.4	1.8×10^{7}	6.8	49	57
20.0,0.0,32.4	1.1×10^{7}	5.0	31	36
25.0,0.0,32.4	7.7×10^{6}	2.9	21	24
30.0,0.0,32.4	5.6×10^{6}	2.2	16	18
35.0,0.0,32.4	4.3×10^{6}	1.7	12	14
40.0,0.0,32.4	3.4×10^{6}	1.3	9.8	11
45.0,0.0,32.4	2.8×10^{6}	1.1	8.1	9.2

Table 12. ^{11}C concentrations (Bq/m^3) and doses ($\mu Sv/a$) in normal release. The total dose at each point of observation was found by adding up the internal and external doses

Point of observation (x,y,z)	C (Bq/m^3)	D (μSv)	E (μSv)	D+E (μSv)
137.4,0.0,0.0	610	0.013	0.097	0.11
137.4,10.0,0.0	560	0.012	0.090	0.10
137.4,20.0,0.0	440	0.0096	0.070	0.080
137.4,30.0,0.0	290	0.0064	0.047	0.053
137.4,40.0,0.0	170	0.0036	0.027	0.030
137.4,50.0,0.0	80	0.0017	0.013	0.015
137.4,60.0,0.0	33	0.00071	0.0052	0.0059
137.4,70.0,0.0	11	0.00025	0.0018	0.0021
137.4,80.0,0.0	3.4	0.000073	0.00054	0.00061
137.4,90.0,0.0	0.85	0.000018	0.00014	0.00015
113.2,0.0,5.0	860	0.019	0.14	0.15
113.2,10.0,5.0	770	0.017	0.12	0.14
113.2,20.0,5.0	550	0.012	0.087	0.098
113.2,30.0,5.0	310	0.0067	0.049	0.056
113.2,40.0,5.0	140	0.0030	0.022	0.025
113.2,50.0,5.0	50	0.0011	0.0080	0.0091
113.2,60.0,5.0	14	0.00031	0.0023	0.0026
113.2,70.0,5.0	3.3	0.000072	0.00053	0.00060
113.2,80.0,5.0	0.61	0.000013	0.000096	0.00011
89.6,0.0,10.0	1.3×10^{3}	0.028	0.20	0.23
89.6,10.0,10.0	1.1×10^{3}	0.024	0.17	0.20
89.6,20.0,10.0	650	0.014	0.10	0.12
89.6,30.0,10.0	280	0.0061	0.045	0.051
89.6,40.0,10.0	86	0.0019	0.014	0.015
89.6,50.0,10.0	19	0.00040	0.0030	0.0034
89.6,60.0,10.0	2.9	0.000062	0.00046	0.00052
45.1,0.0,20.0	4.2×10^{3}	0.092	0.67	0.77
45.1,10.0,20.0	2.4×10^{3}	0.053	0.39	0.44
45.1,20.0,20.0	460	0.010	0.074	0.084
45.1,30.0,20.0	29	0.00063	0.0046	0.0011
45.1,40.0,20.0	0.61	0.000013	0.000097	0.00011
45.1,50.0,20.0	0.0042	4.0×10^{-7}	6.7×10^{-7}	7.6×10^{-7}
5.0,0.0, 32.4	2.5×10^{5}	5.6	41	41
5.0,10.0, 32.4	3.3×10^{-6}	7.2×10^{-11}	5.3×10^{-10}	6.0×10^{-10}
10.0,0.0,32.4	1.4×10^{5}	3.1	23	26
15.0,0.0,32.4	7.6×10^{4}	1.7	12	14
20.0,0.0,32.4	4.7×10^{4}	1.0	7.5	8.5

Table 13. ^{18}F concentrations (Bq/m^3) and doses (μSv/a) in normal release. The total dose at each point of observation was found by adding up the internal and external doses

Point of observation (x,y,z)	C (Bq/m^3)	D (μSv)	E (μSv)	D+E (μSv)
138.2,0.0,0.0	210	0.0094	0.033	0.042
138.2,10.0,0.0	200	0.0087	0.030	0.039
138.2,20.0,0.0	150	0.0068	0.024	0.031
138.2,30.0,0.0	100	0.0046	0.016	0.021
138.2,40.0,0.0	59	0.0026	0.0091	0.012
138.2,50.0,0.0	29	0.0013	0.0044	0.0057
138.2,60.0,0.0	12	0.00053	0.0018	0.0024
138.2,70.0,0.0	4.2	0.00018	0.00064	0.00083
138.2,80.0,0.0	1.2	0.000055	0.00019	0.00025
138.2,90.0,0.0	0.32	0.000014	0.000049	0.00064
113.7,0.0,5.0	300	0.013	0.046	0.059
113.7,10.0,5.0	270	0.012	0.041	0.053
113.7,20.0,5.0	190	0.0084	0.029	0.038
113.7,30.0,5.0	110	0.0048	0.017	0.0.022
113.7,40.0,5.0	49	0.0022	0.0076	0.0098
113.7,50.0,5.0	18	0.00080	0.0028	0.0036
113.7,60.0,5.0	5.2	0.00023	0.00081	0.0010
113.7,70.0,5.0	1.2	0.000054	0.00019	0.00024
89.9,0.0,10.0	450	0.020	0.069	0.089
89.9,10.0,10.0	380	0.017	0.058	0.075
89.9,20.0,10.0	230	0.010	0.035	0.045
89.9,30.0,10.0	98	0.0043	0.015	0.020
89.9,40.0,10.0	30	0.0013	0.0047	0.0060
89.9,50.0,10.0	6.7	0.00029	0.0010	0.0013
89.9,60.0,10.0	1.0	0.000046	0.00016	0.00021
45.2,0.0,20.0	1.5×10^3	0.065	0.23	0.29
45.2,10.0,20.0	850	0.037	0.13	0.17
45.2,20.0,20.0	160	0.0072	0.025	0.032
45.2,30.0,20.0	10	0.00046	0.0016	0.0021
5.0,0.0, 32.4	8.8×10^4	3.9	14	18
45.0,0.0, 32.4	2.8×10^6	2.2	8.0	10
50.0,0.0,32.4	2.3×10^6	1.8	6.6	8.4